Computing@CSN5: applications and innovations at INFN

Imaging algorithms for in-vivo BNCT dosimetry

D. Ramos Lopez, N. Ferrara, A. Didonna, G. Pugliese, G. Iaselli

dayron.ramos@ba.infn.it

Outline

- State of art of BNCT
- **Part1:** Dose monitoring by Single Photon Emission Computational Tomography (SPECT)
  - SPECT project
  - Simulation and reconstruction algorithm development
- **Part2:** Dose monitoring by Compton imaging
  - Compton imaging principles
  - Simulations and classical tomography with iteratives algorithms
  - Novel approach by Deep Learning (DL) models
- Summary and future

Boron neutron capture therapy

Boron Neutron Capture Therapy (BNCT) is an innovative hadrontherapy with high selectivity over cancer tissue based on the neutron capture reaction $^{10}B(n, \alpha)7Li$

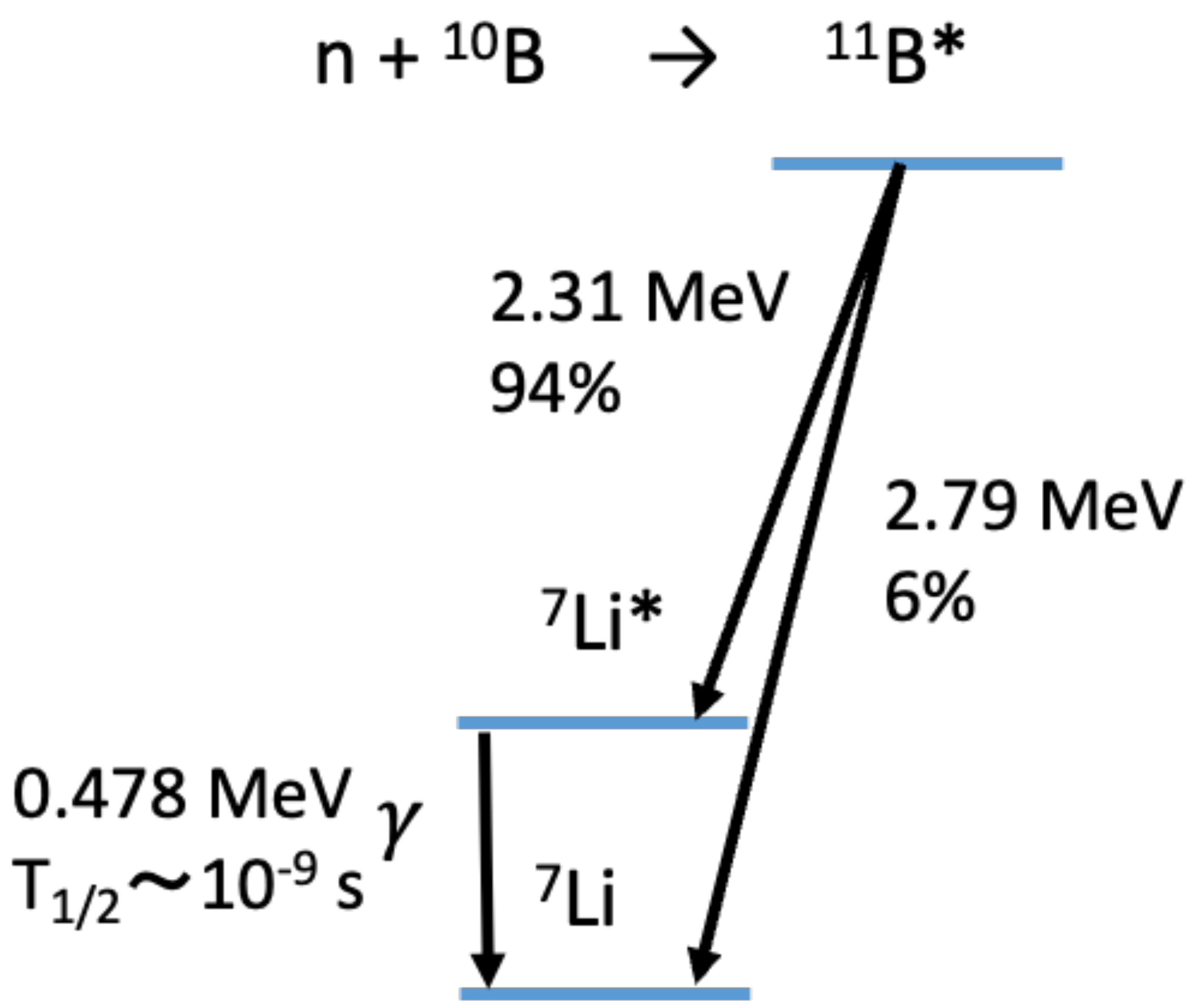

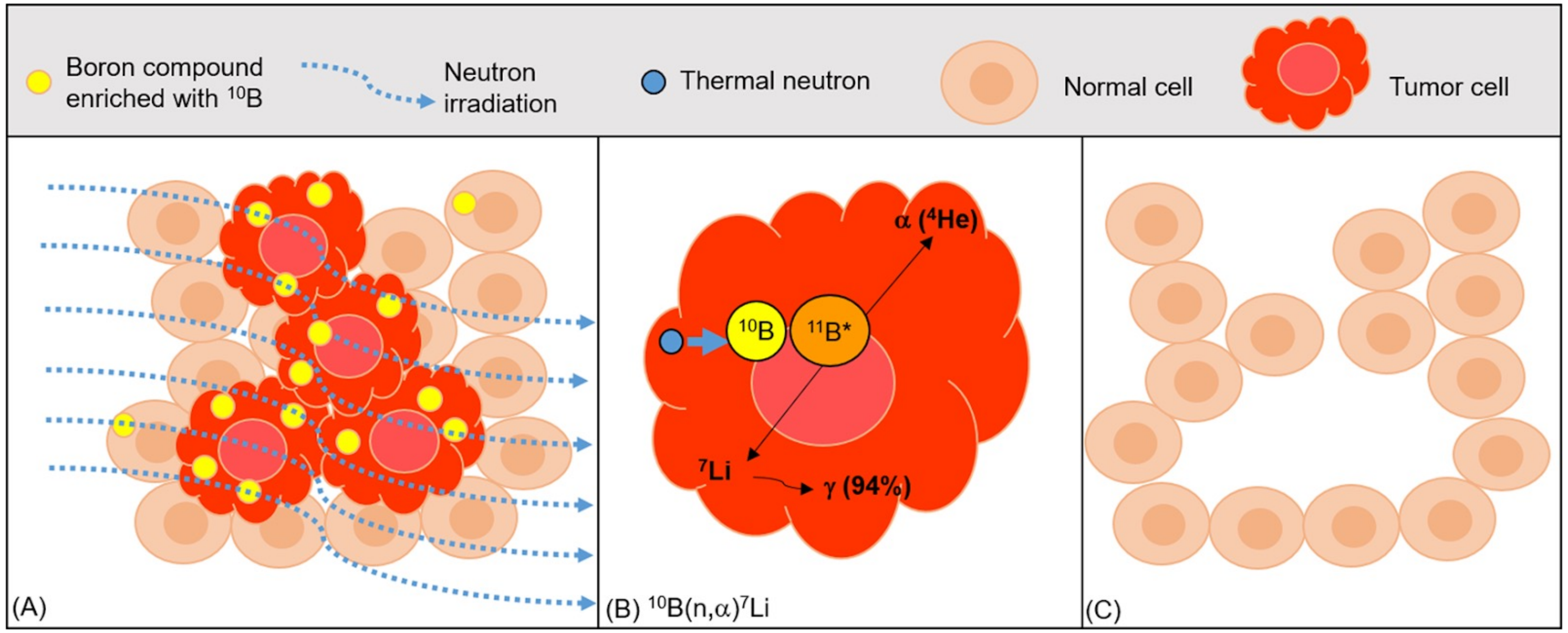

	Energy (MeV)	Range (µm)
α	1.47-178	9-11
^{7}Li	0.84-101	4-5
γ	0.48	

- Dose distribution: $dD(x,y,z) \approx n_{^{10}B}(x,y,z)\ \Phi(x,y,z)\ dV$
- Reaction products range < cell dimensions (≈ 10 µm) → **high selectivity**
- Tumor-to-healthy boron concentration ratio (T/N) > 3*.
- Treatment duration ≈30-90 min

*Skwierawska, D. et. al. Clinical Viability of Boron Neutron Capture Therapy for Personalized Radiation Treatment. Cancers 2022, 14, 2865.

Dosimetry on BNCT

- Main nuclear interactions that contribute to the BNCT total dose delivery:

D_{total} =

D_B Therapeutic dose from $^{10}B(n,\alpha)^{7}Li$ (σ=3837 b)

+ D_p From $^{14}N(n,p)^{14}C$ reactions (Ep=630 keV, σ=1.9 b) due to thermal neutron

+ D_n Due to epithermal and fast neutron elastic scattering daily with H nuclei

+ D_γ From $^{1}H(n,\gamma)^{2}H$ (E=2.2 MeV, σ=0.33 b) & reactor background

→ Therapeutic boron dose as main dose contributor.

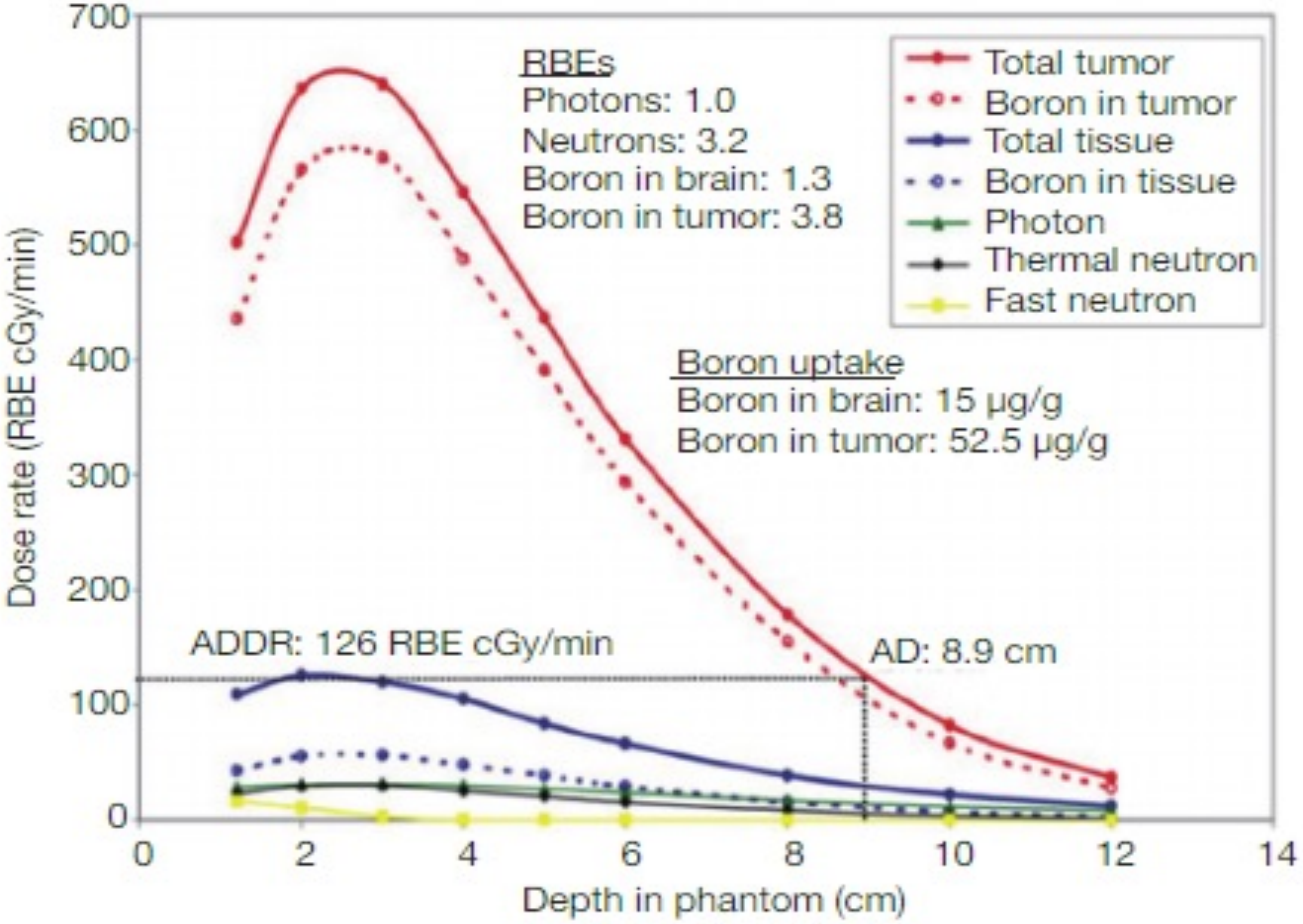

Altieri S, Protti N. A brief review on reactor-based neutron sources for boron neutron capture therapy. Ther Radiol Oncol 2018;2:47.

Dosimetry on BNCT

Nowadays dose estimation in BNCT:

- by blood test before, meanwhile and after irradiation, and
- Monte Carlo simulations to estimate all dose delivery contributes and neutron capture rates

Proposal:

Development of an **on-line boron dose estimation algorithm** by using **Compton imaging** and/or **Single Photon Emission Computational Tomography (SPECT)**

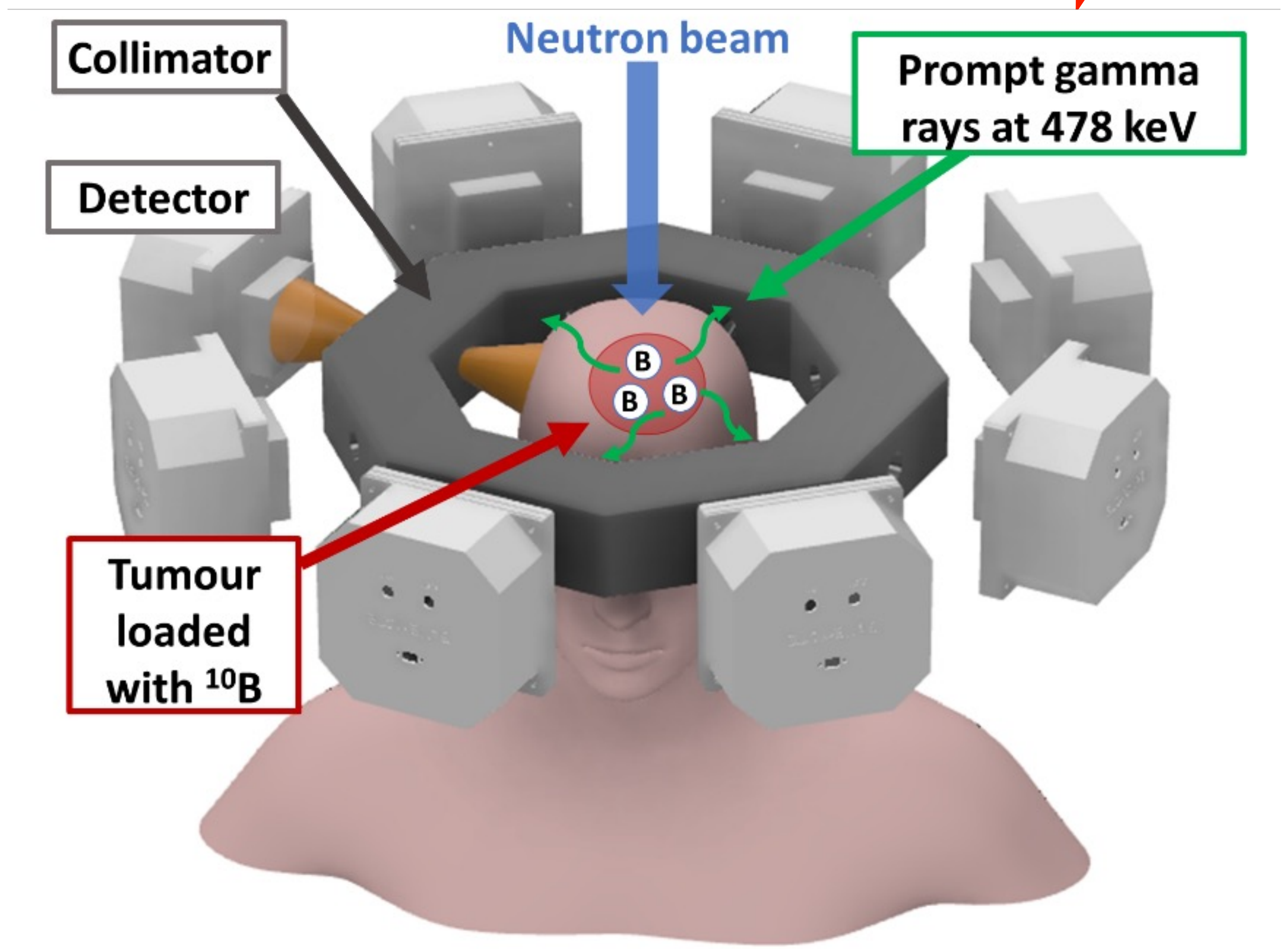

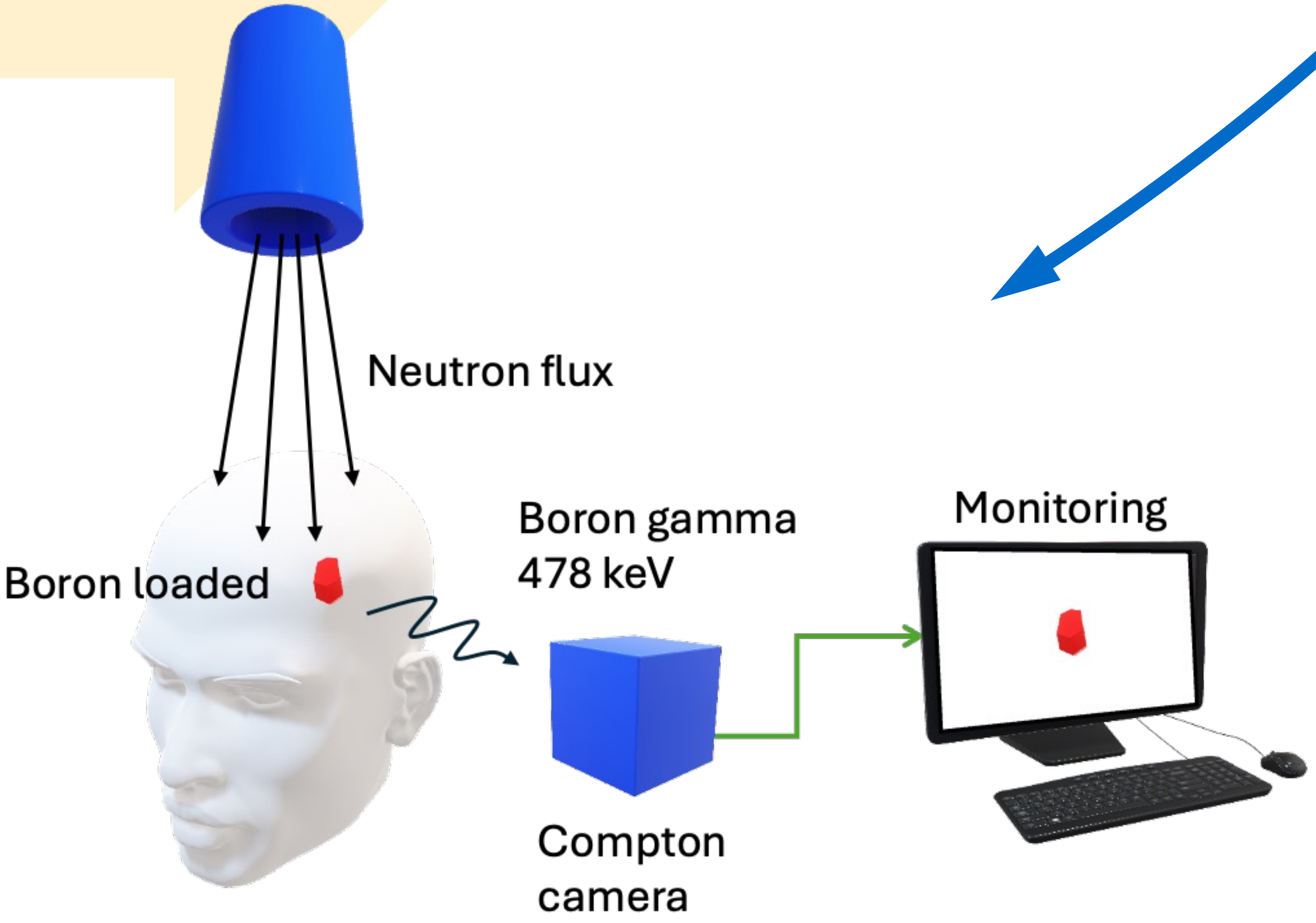

Dose monitoring by SPECT

SPECT system

System based on BeNEdiCTE (Boron Neutron CapTurE) detector: Gamma ray detection module based on a **$LaBr_3$(Ce+Sr) scintillator crystal** readout by **Silicon Photomultipliers** and compact electronics with **ASICs and FPGA**.

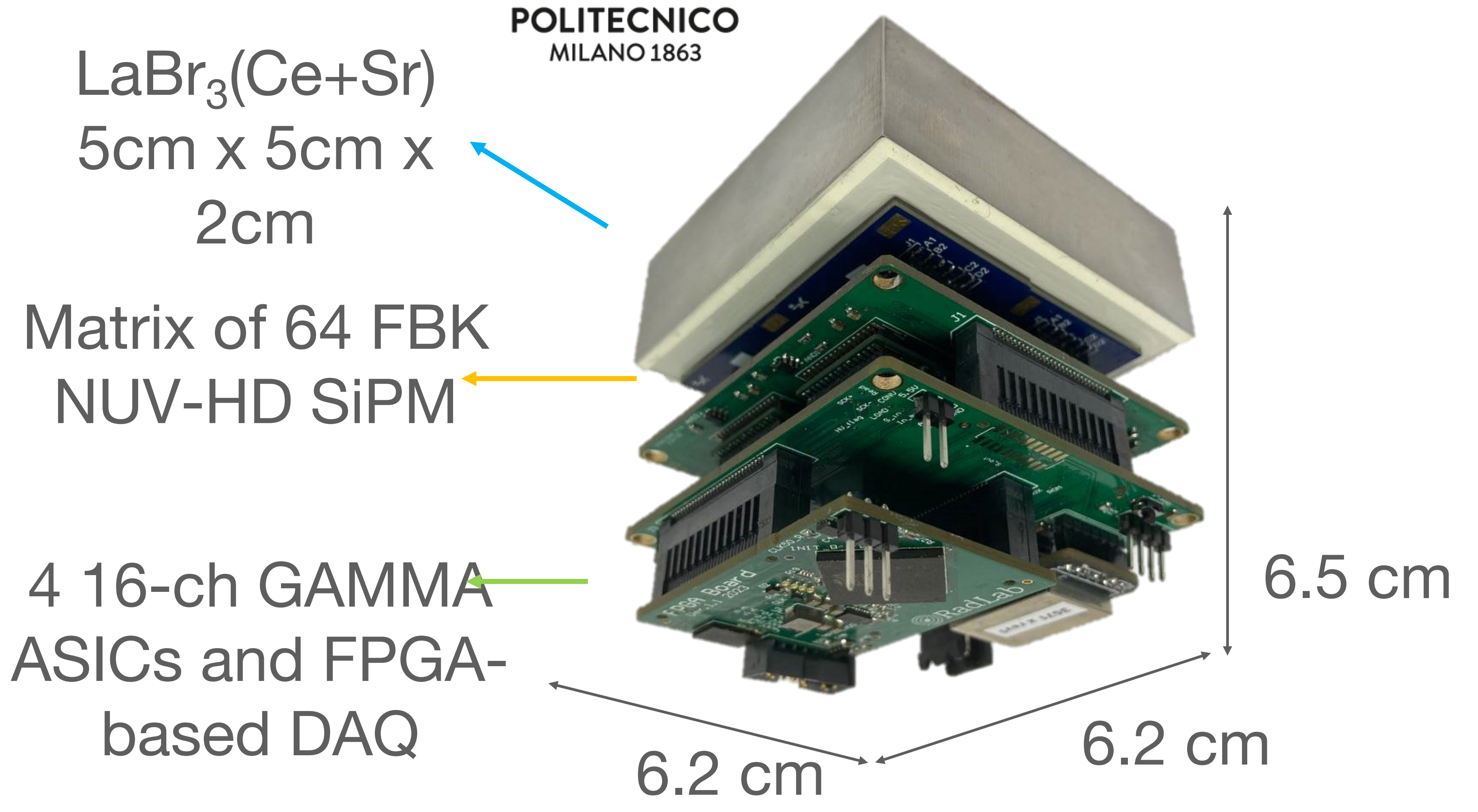

- Founded by INFN CSN5
- "SPOC: SPect for Online boron dose verification in bnCt" and PRIN-2024 PNRR*
- Bari unit → Development of BNCT-SPECT dedicated tomography reconstruction

We are here!

Geant4 simulation → Implementation of classic tomography methods (OSEM) → Model validation with simulated and experimental data → Tomography improvement by Deep Learning tools

* Collaboration with UNIPV and POLIMI, and INFN sections

Monte Carlo simulations

- Monte Carlo simulation performed in ideal conditions (no background from facility) for first data availability
- Pure irradiated boron gamma source
- Layout based on experimental setup at Nagoya

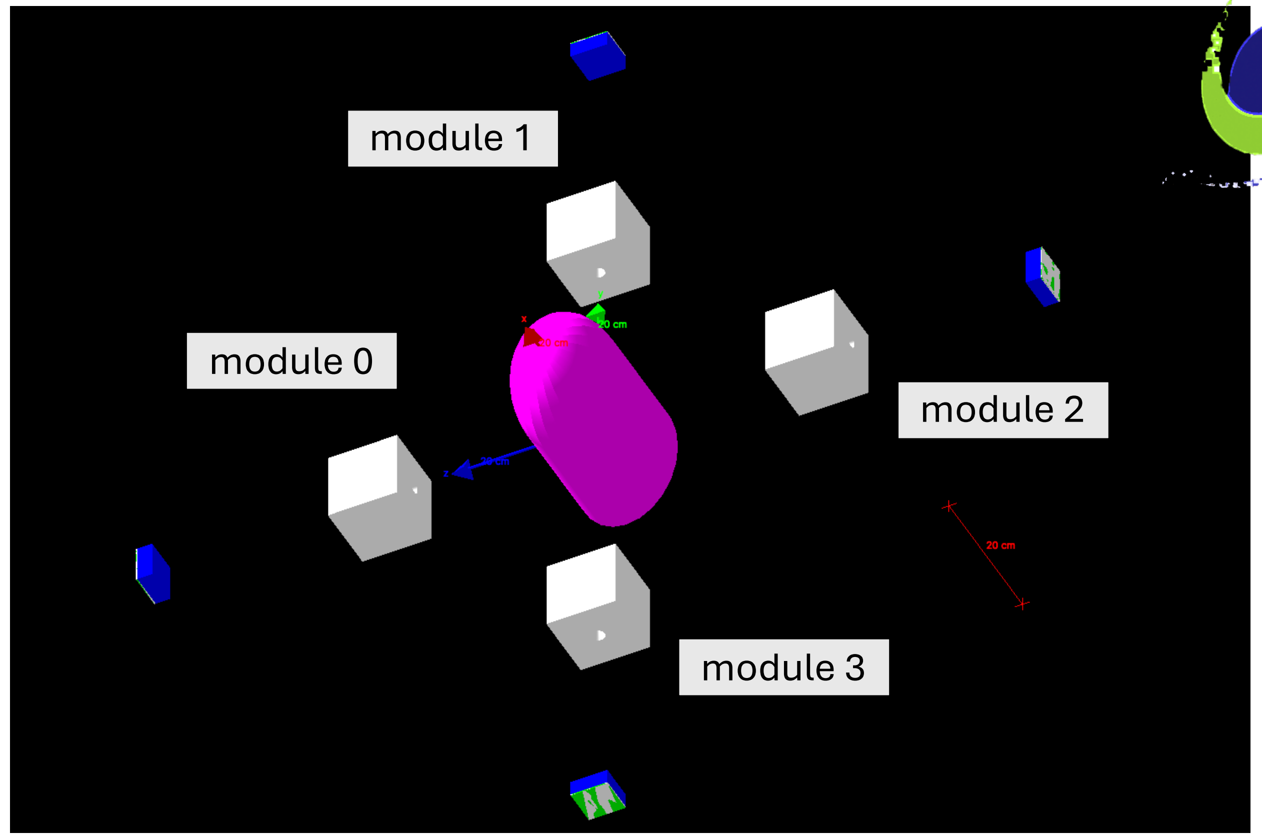

Polimi pinhole collimator: Pb

Scintillator crystal: $LaBr_3$ (5 x 5 x 2 cm^3)

SiPM: 8x8 array (5 x 5 x 0.2 cm^3)

Human head: G4_TISSUE_SOFT_ICRP

1 modules → 4 modules → 16 modules

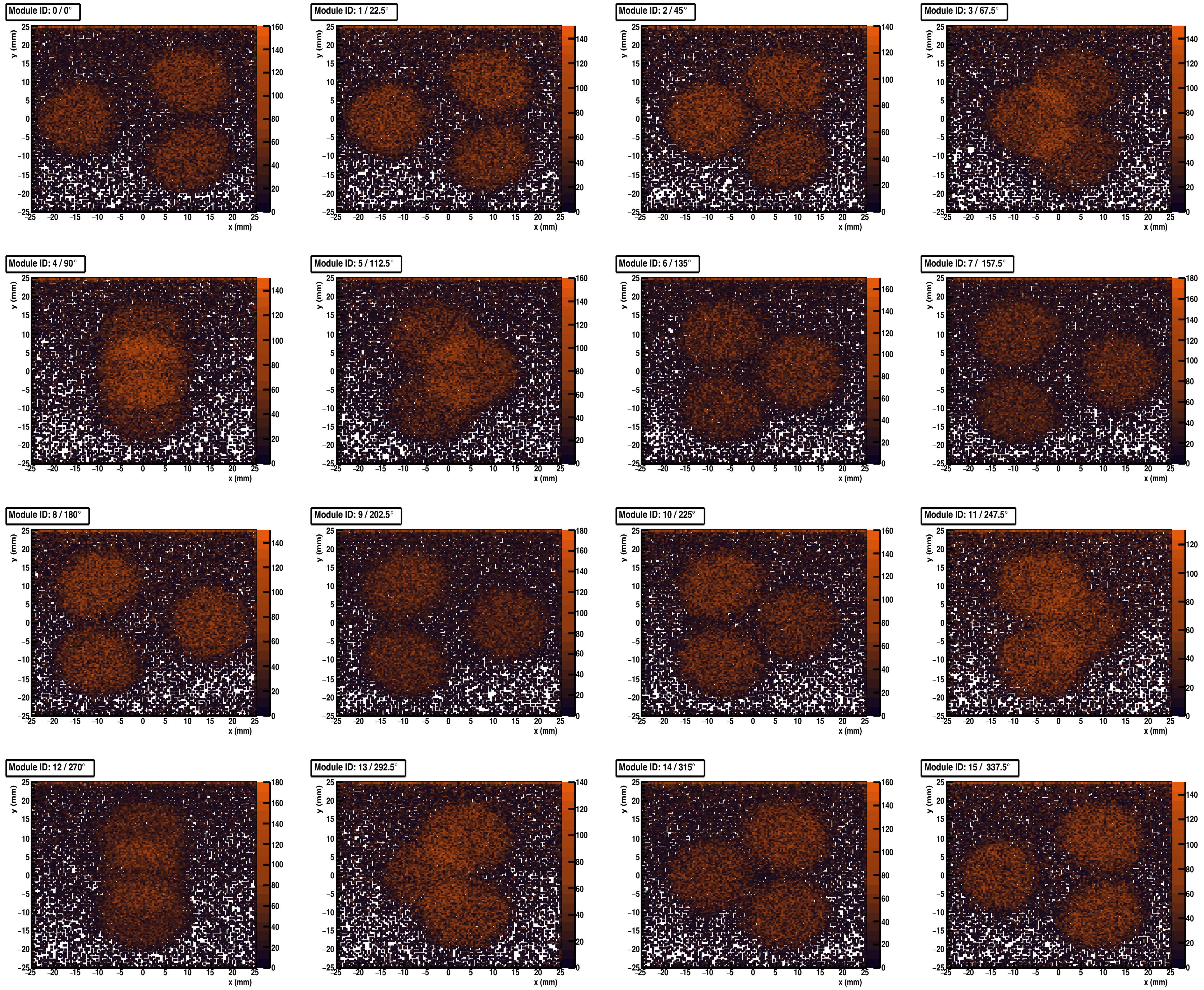

Detector projections: 3 spheres 2.5 mm radius, centered 15 mm apart from the center in the same plane

Tomography reconstruction

Based on PyTomography libraries with the iterative method: Ordered Subset Expectation Maximum(**OSEM**) on GPU-accelerated

$$\lambda(\text{new})_j = \frac{\lambda(\text{old})_j}{\sum_{D_n}\sum_{D_m}\sum_{i\in S_L} C_{ij(nm)}} \times \sum_{D_n}\sum_{D_m}\sum_{i\in S_L} C_{ij(nm)} \left(\frac{Y_{i(nm)}}{\sum_K C_{ik(nm)}\lambda(\text{old})_k} \right),$$

where λ = image variable, C_{ij} = system matrix, Y_i = Count number of photon, D_n = GPU domain length (horizontal thread number), and D_m = GPU domain length (vertical thread number).

Collimator resolution function

$$R_{coll} = \left(\frac{x}{f}\right)\sqrt{R_d^2 + \left(\frac{f+x}{x+\frac{CH}{2}}\right) * d_e^2}$$

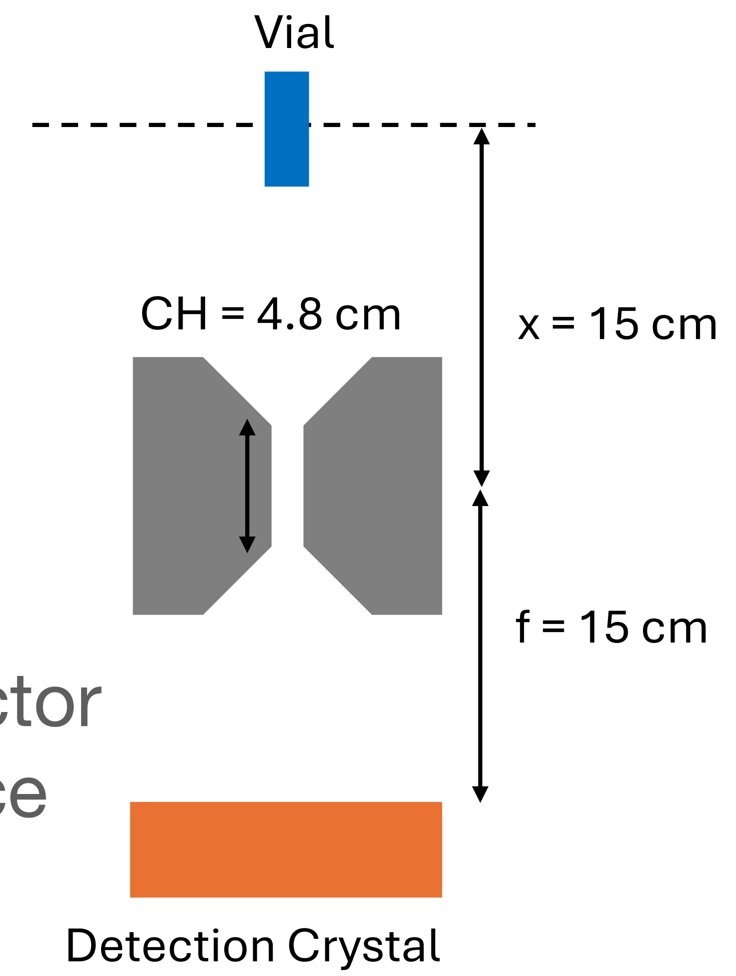

R_d = 3.0 mm, intrinsic resolution
f = 15 cm, distance collimator-detector
x = 15 cm, distance collimator-source
d_e = 5 mm, pinhole diameter
CH = 48.04 mm, channel length

Preliminary tomography

- iterations: 50, subsets: 3
- Pixel side: 0.39 mm
- Spheres reconstructed with ∽ **2.5 mm radius in agreement with simulated configuration**

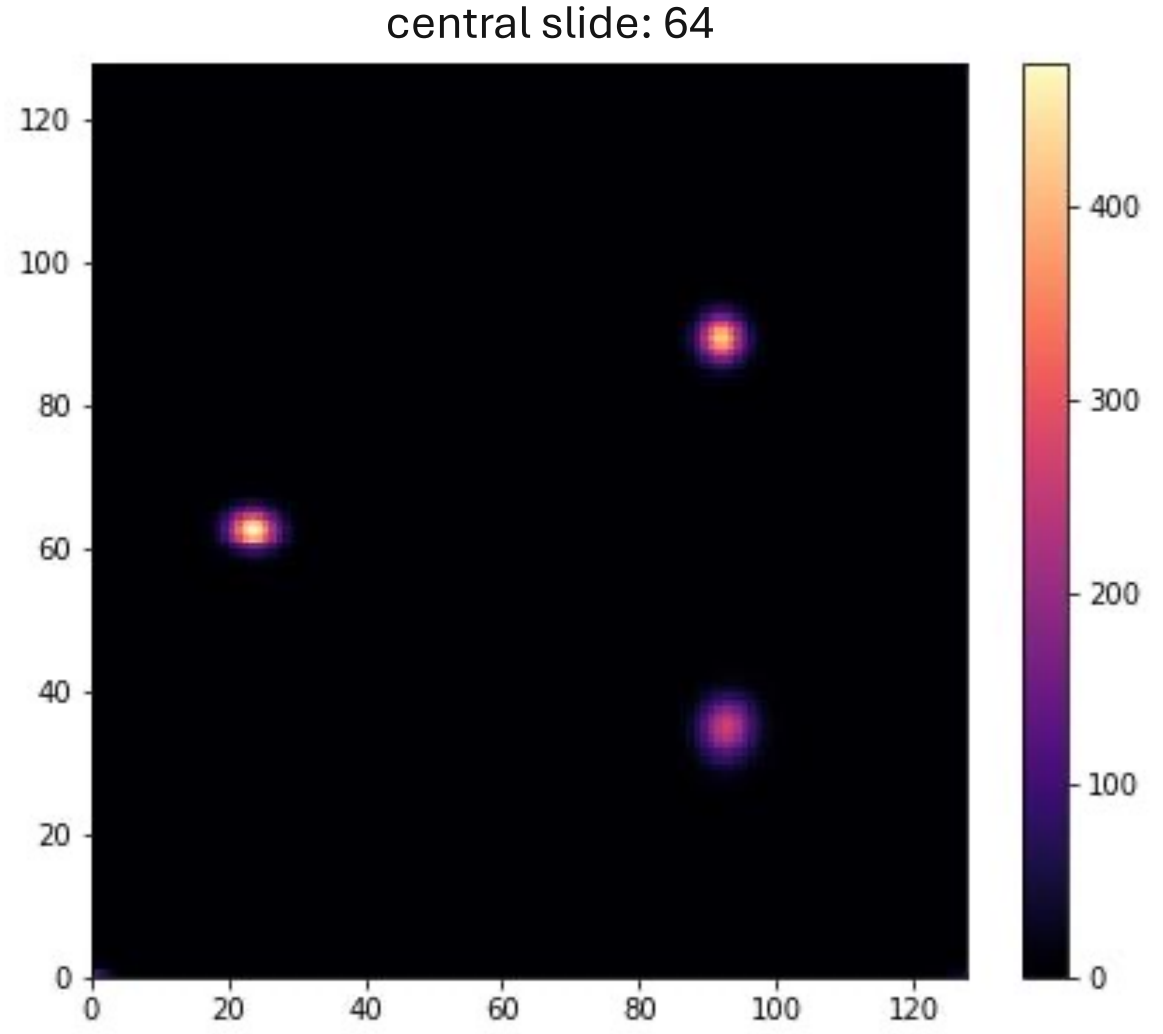

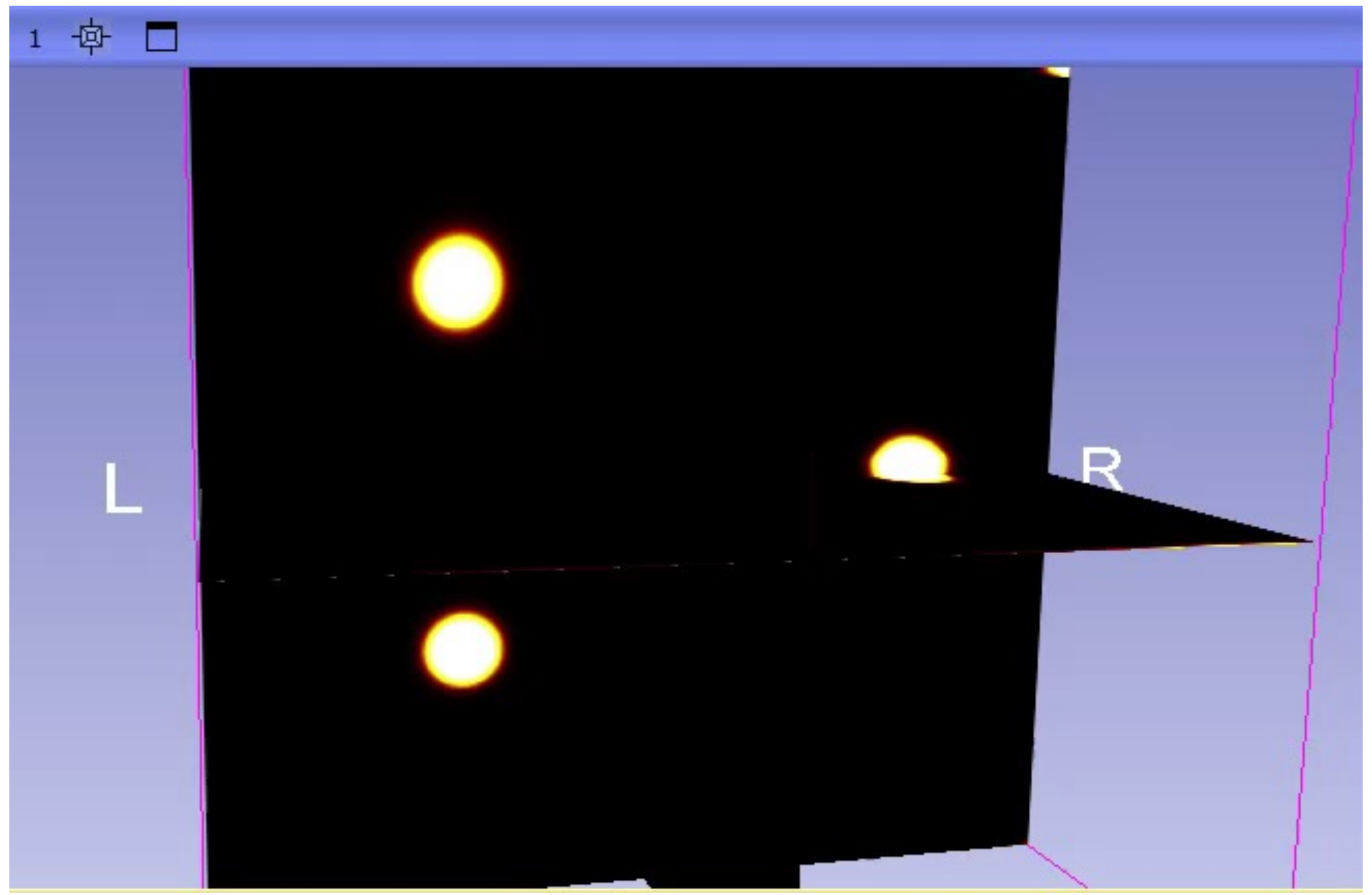

Tomography reconstruction

Algo. validation with Vials Tomography reconstruction

Simulated Polimi dataset describing a more realistic treatment conditions adapted to LENA set-up

Two Vials

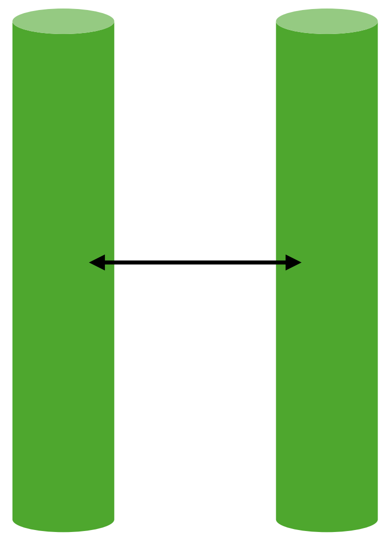

10 mm

- 6 projections **(Polimi dataset "ideal")**
- Difference angle: 60°
- Last resolution function
- Energy range 465-490 keV
- Ideal projections

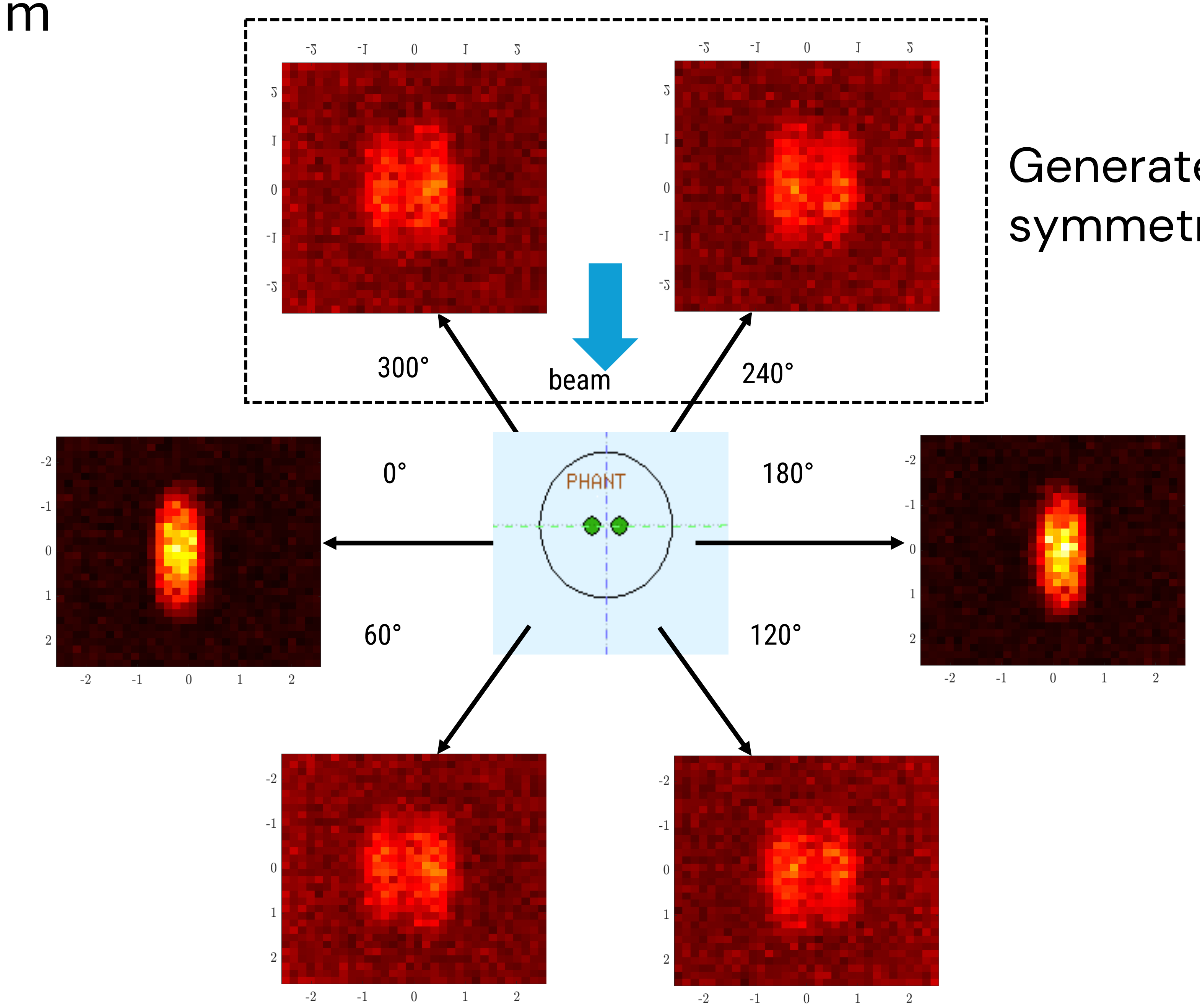

Reconstruction

- iterations: 100, subsets: 3 by **OSEM pytomography**
- Pixel side: 0.32 mm
- Vials reconstructed with ∽ **10 mm distance**

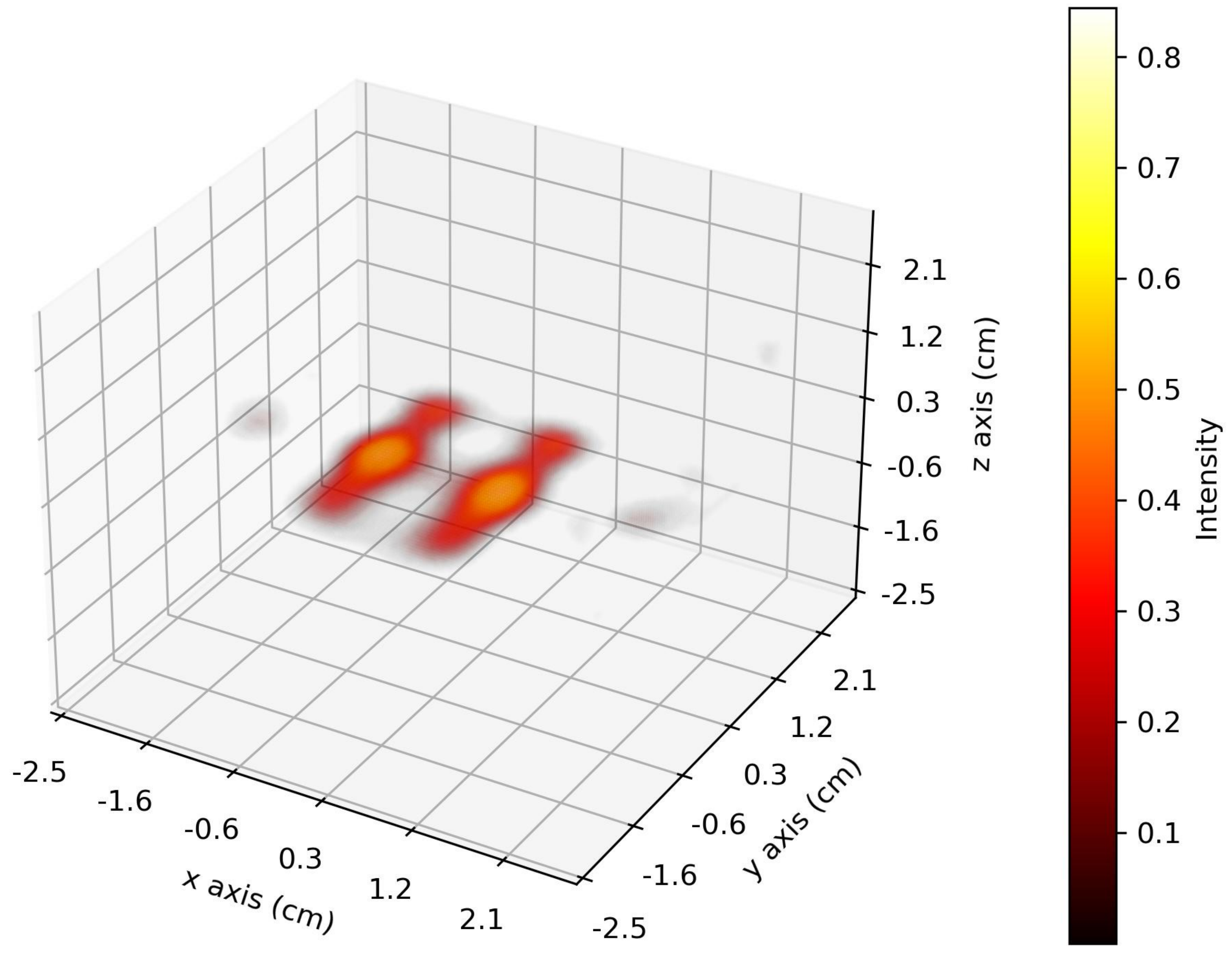

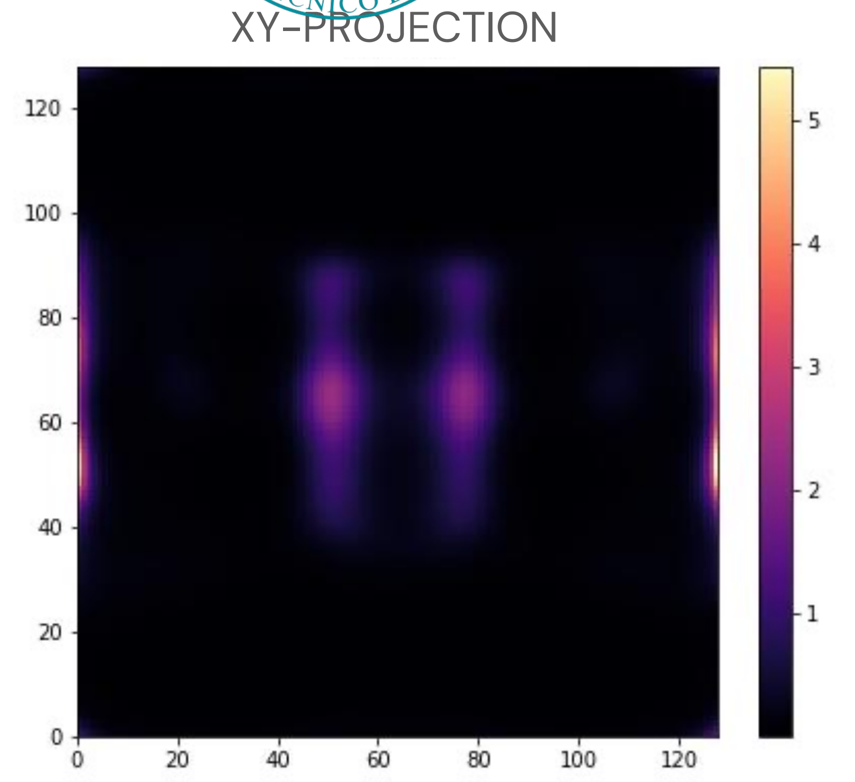

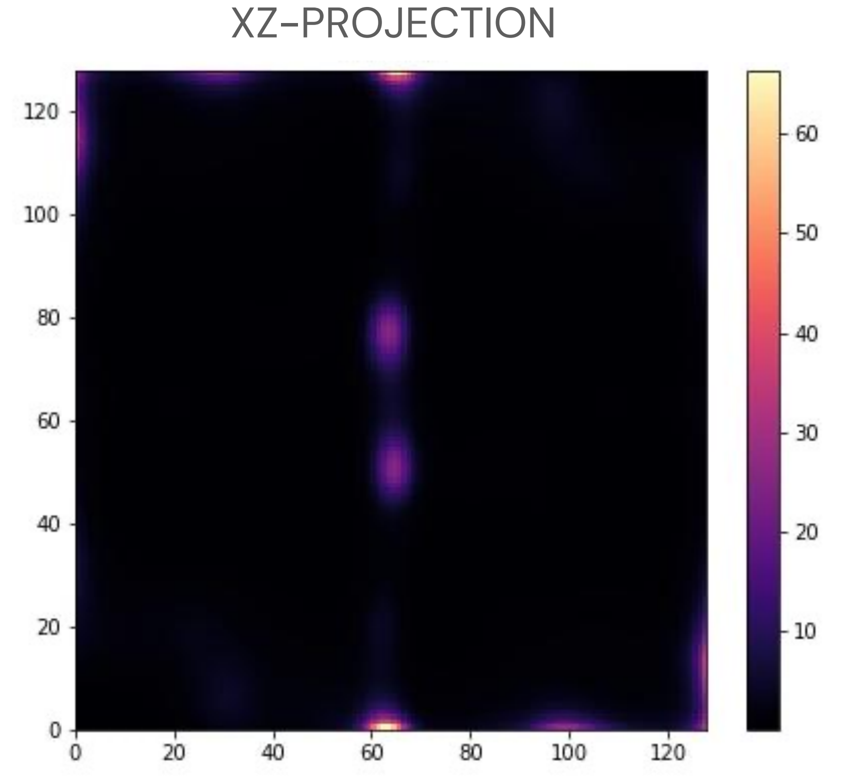

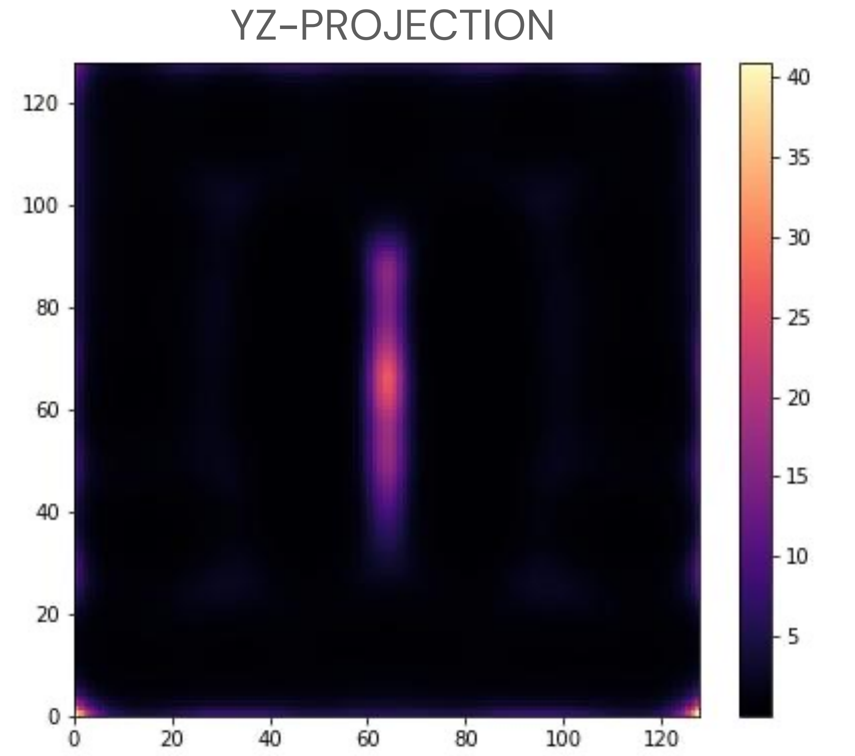

Dose monitoring by Compton imaging

Istituto Nazionale di Fisica Nucleare
Sezione di Bari

Compton imaging principles

- **Principle**

$$cos(\theta) = 1 - m_e c^2 \left(\frac{1}{E_a} - \frac{1}{E_\gamma}\right)$$

where $E_\gamma = E_s + E_a$

→ Compton event: the position of the source is confined in the Compton cone and found by overlapping them

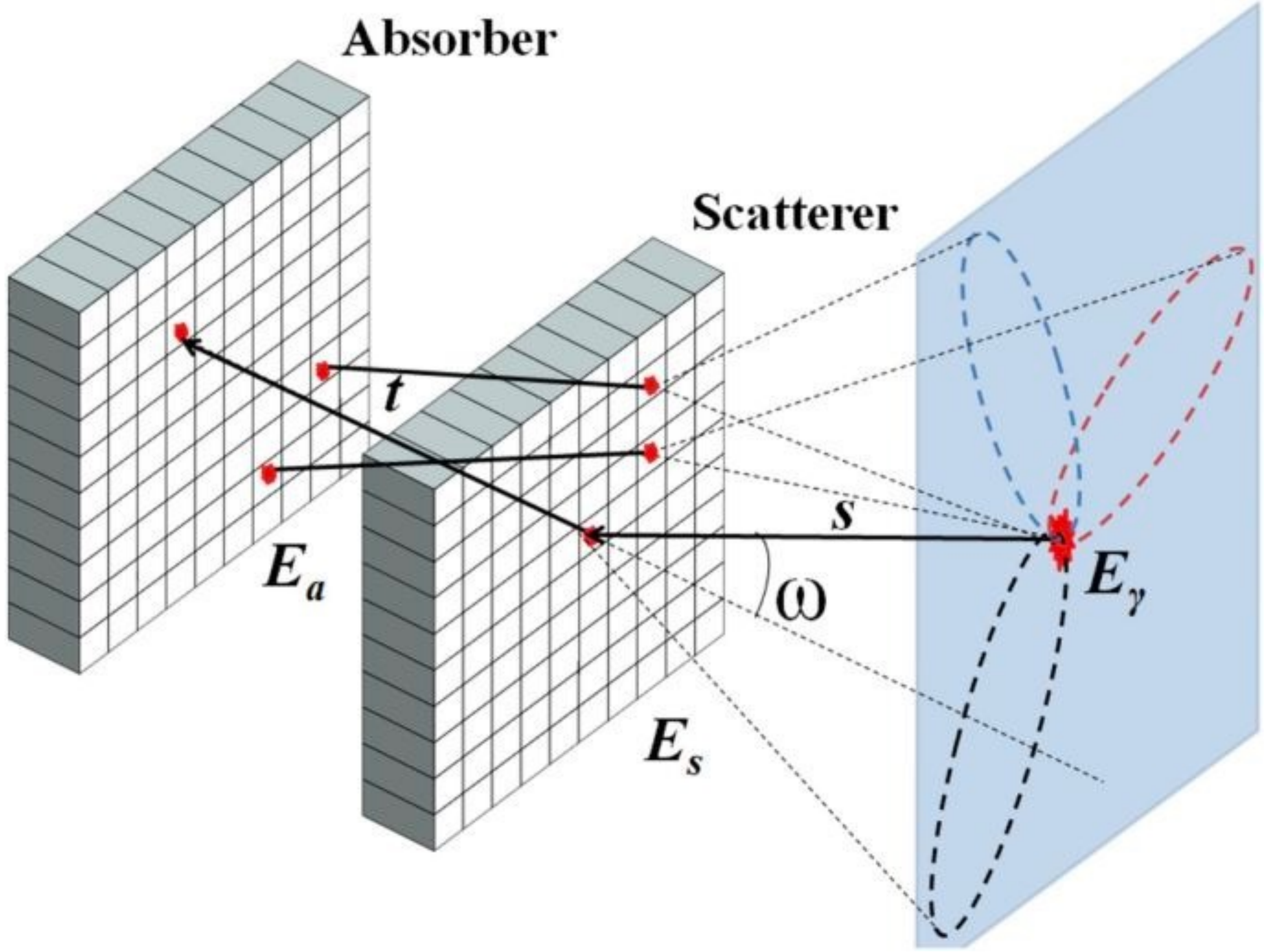

- **Single stage Compton imaging or "True events"**
  good events don't include multiscattering Compton
- **Main advantages: 1)** Reconstruction noise-resolution **2)** Detection sensitivity gain of the order of 30 – 600 with respect to mechanically collimated systems
- Complex reconstruction by classical algorithms, high computational cost

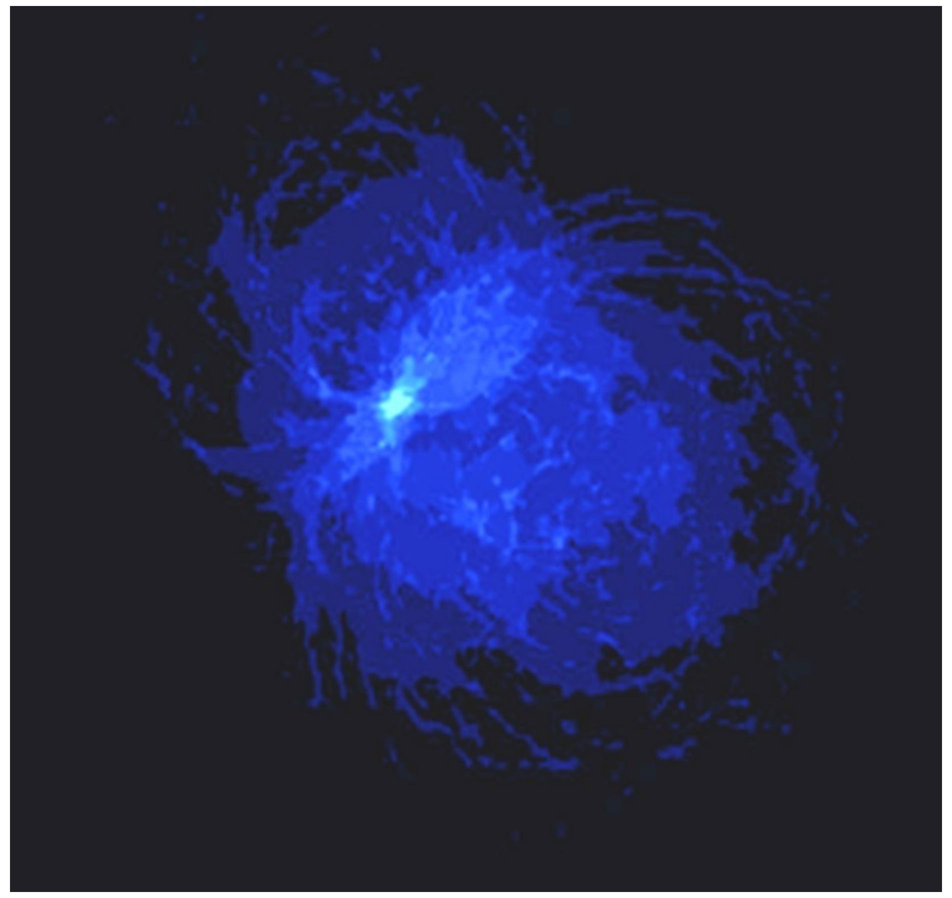

Backward projection example

Preliminary simulation set-up

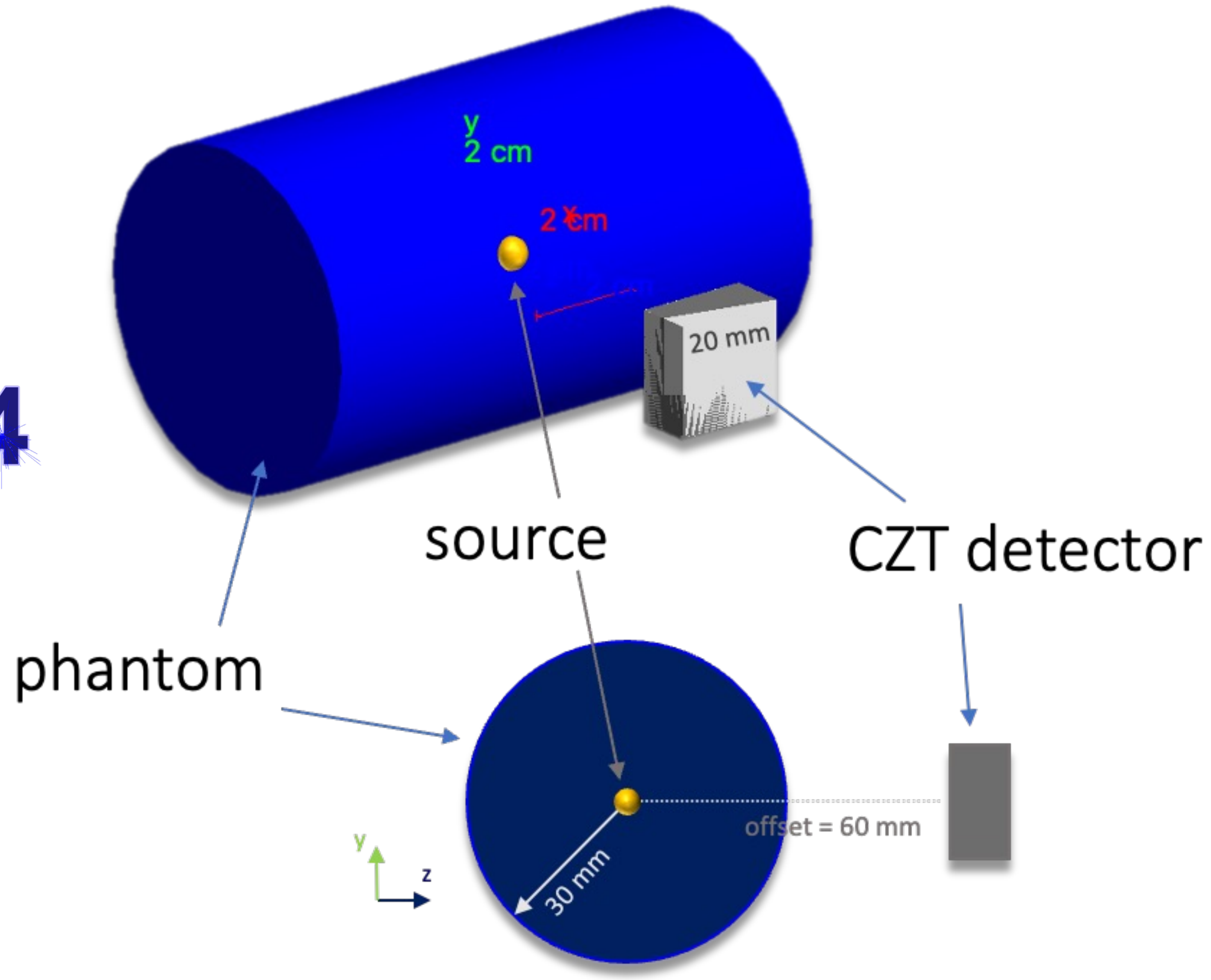

- Detector: CZT crystal stack (5 mm thickness each), 60 mm from the source
- Phantom material: Air, soft tissue
- Simulated sources: 5-points like and spheric 478 keV gamma distributions

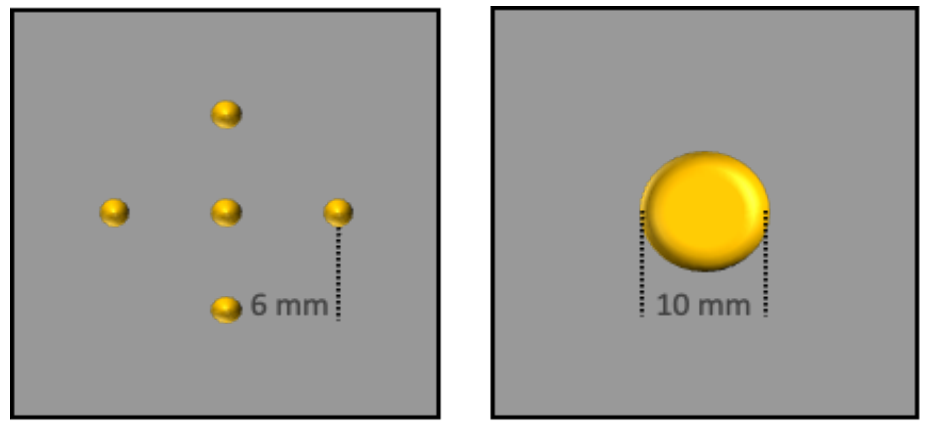

- Tomography FOV: cube 120 mm side centered with source and covering the entire phantom.

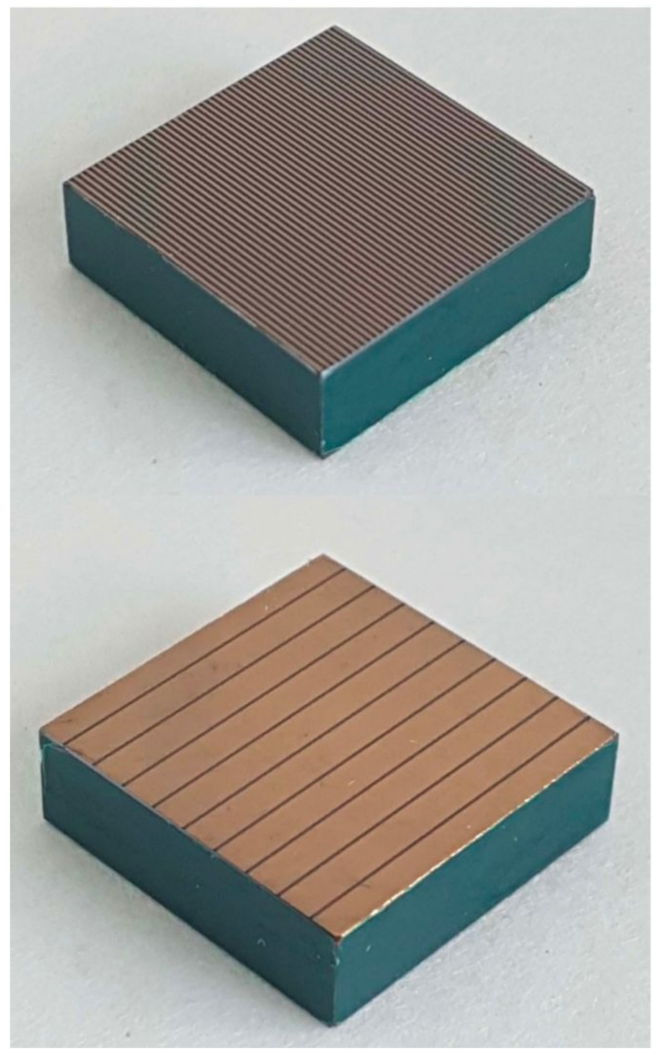

Detector simulated inspired in **CZT sensor by Due2Lab**

- Room-temperature gamma-ray spectroscopic
- Sub-millimetre spatial resolution and excellent energy resolution (around 1% FWHM at 661.7 keV)

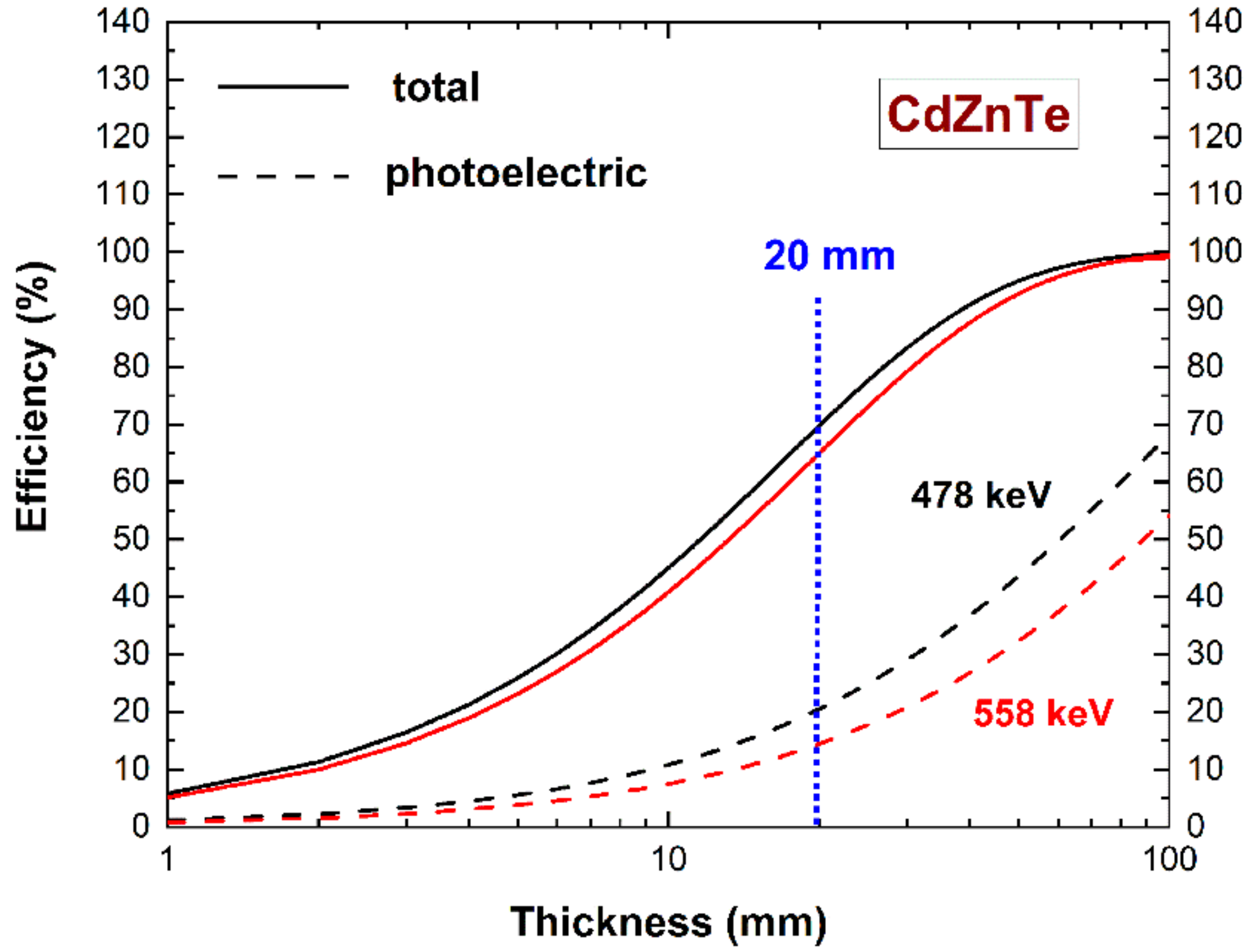

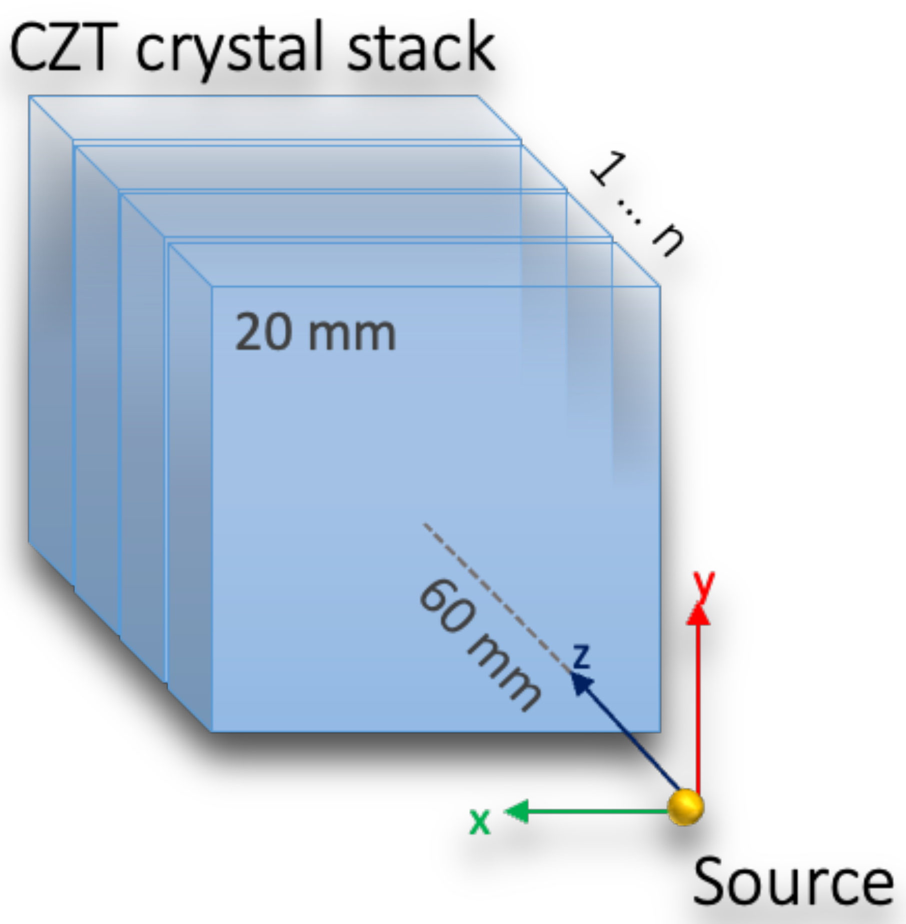

Abbene, L.; Principato, F.; Buttacavoli, A. and et al.: Potentialities of High-Resolution 3-D CZT Drift Strip Detectors for Prompt Gamma-Ray Measurements in BNCT. Sensors, 22, 1502 (2022)

MLEM reconstruction method validation

Maximum Likelihood Expectation Maximisation (MLEM) → Iterative method to reconstruct the most probable source distribution

$$\lambda_j^n = \frac{\lambda_j^{n-1}}{s_j} \sum_{i=1}^{N} \frac{t_{ij}}{\sum_k t_{ik} \lambda_k^{n-1}}$$

- λ^n_j = calculated amplitude of pixel *j* at the nth iteration
- s_j = sensitivity, i.e. the probability that a gamma ray originating from pixel *j* is detected anywhere
- t_{ij} = imaging response matrix, i.e. the transition probabilities generated by the measured events(first estimation: based on back-projection, λ_0)

On Air phantom

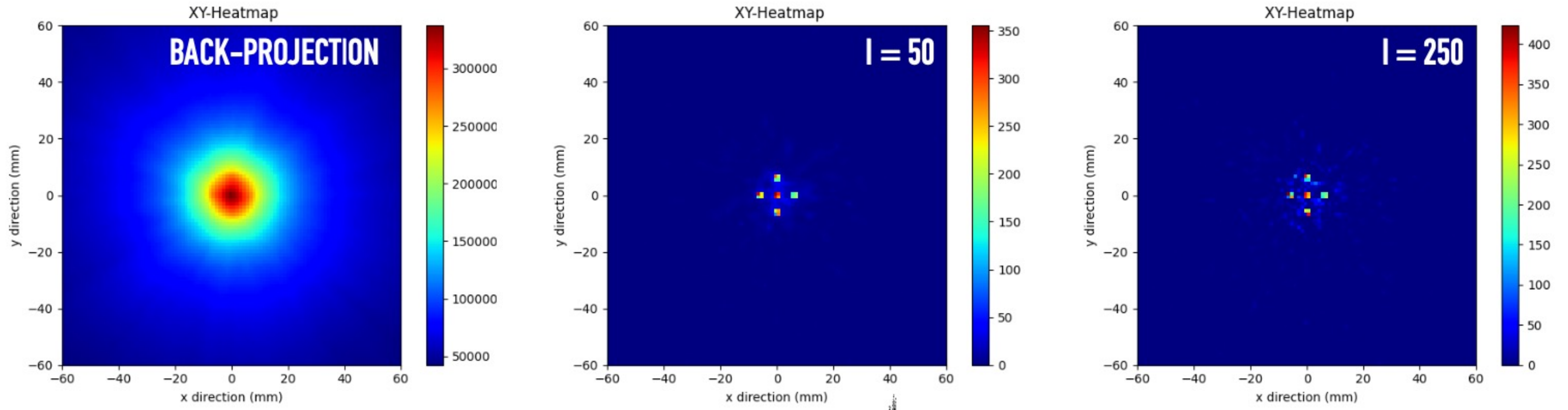

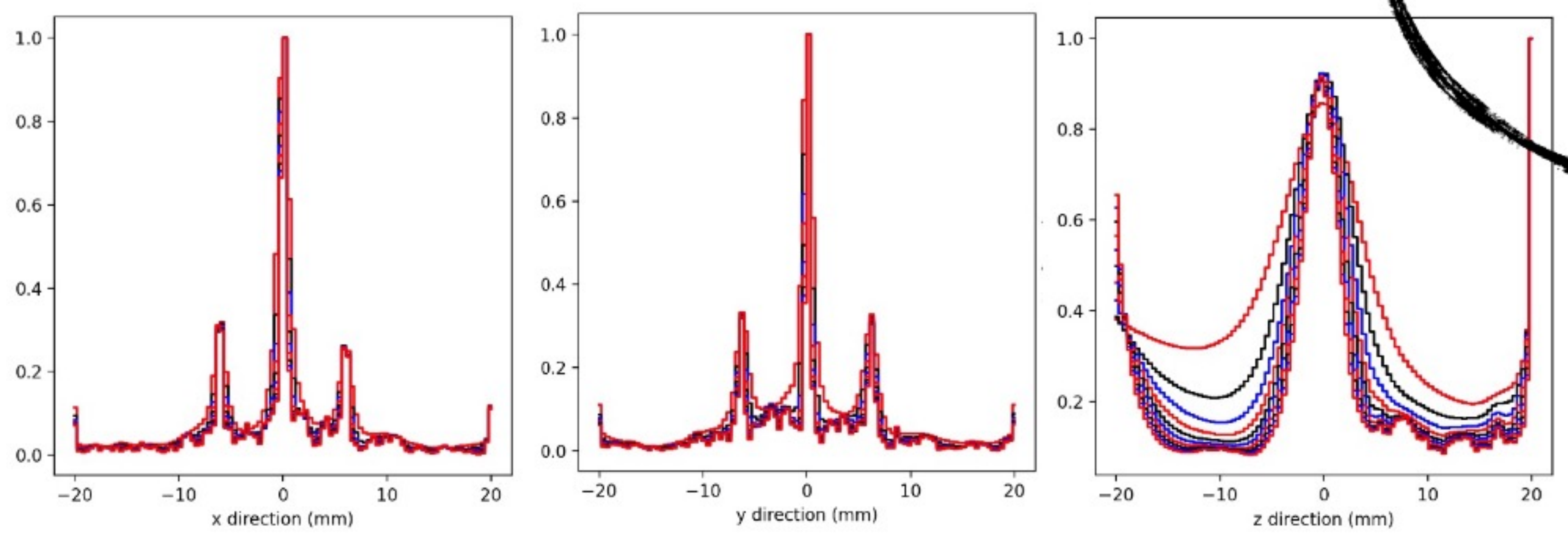

On Tissue phantom

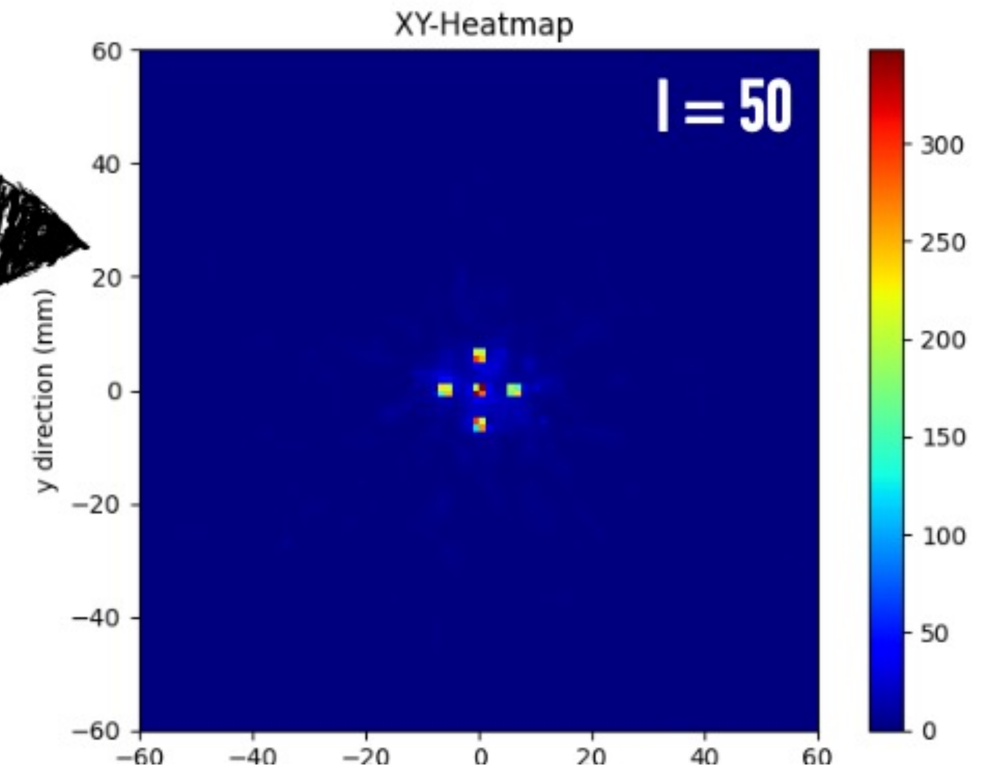

- Good resolution in x and y profiles, slightly worse in z direction (stretching effect)
- No image interference when phantom is added

Tumor-to-healthy 2D boron ratio study

On Tissue phantom, T/N = 5.0

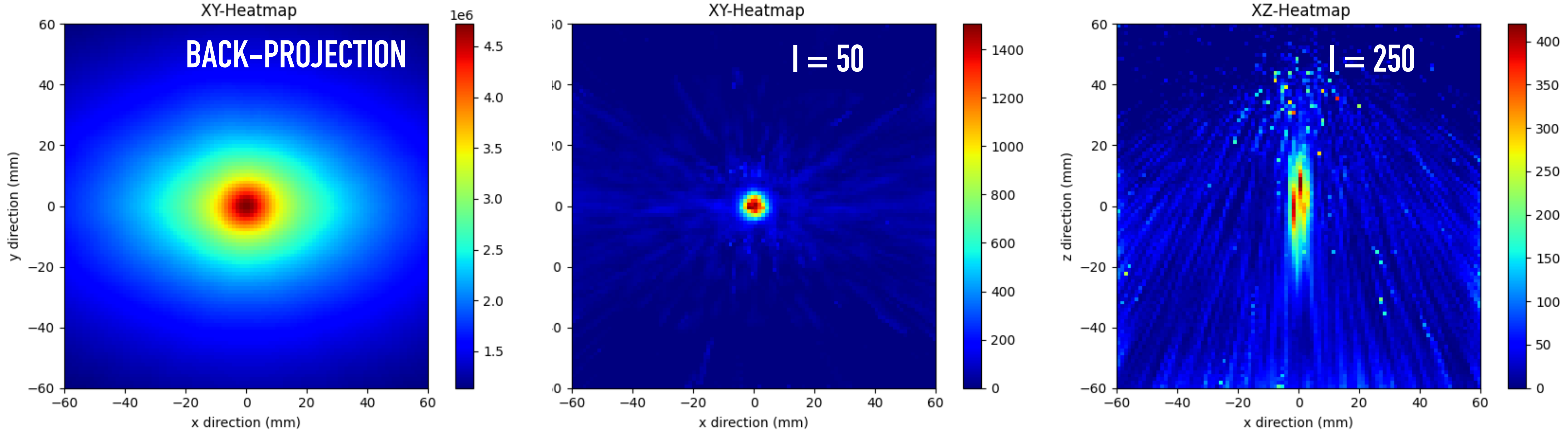

On Tissue phantom, T/N = 2.0

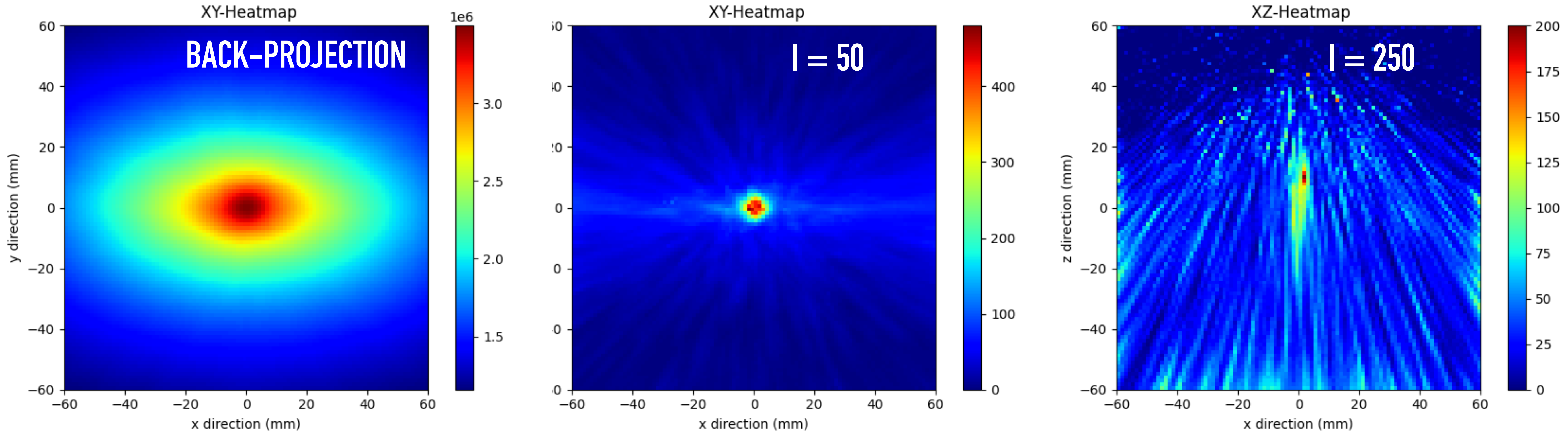

- Spheric source in more realistic conditions
- Two different ratios: **ideal case (T/N = 5)** and **(T/N = 2) extreme case** (clinical values are T/N>3)
- Both distributions resolute.

→ More iterations needed to solve the image in z (≈250)

Iteration methods and novel approach

- **Limitation for online dose measurements:** MLEM works only post-irradiation, computational times ≈24-36 min

- New approach **to go from the back-projection image to the tomography dose by using Deep Learning**

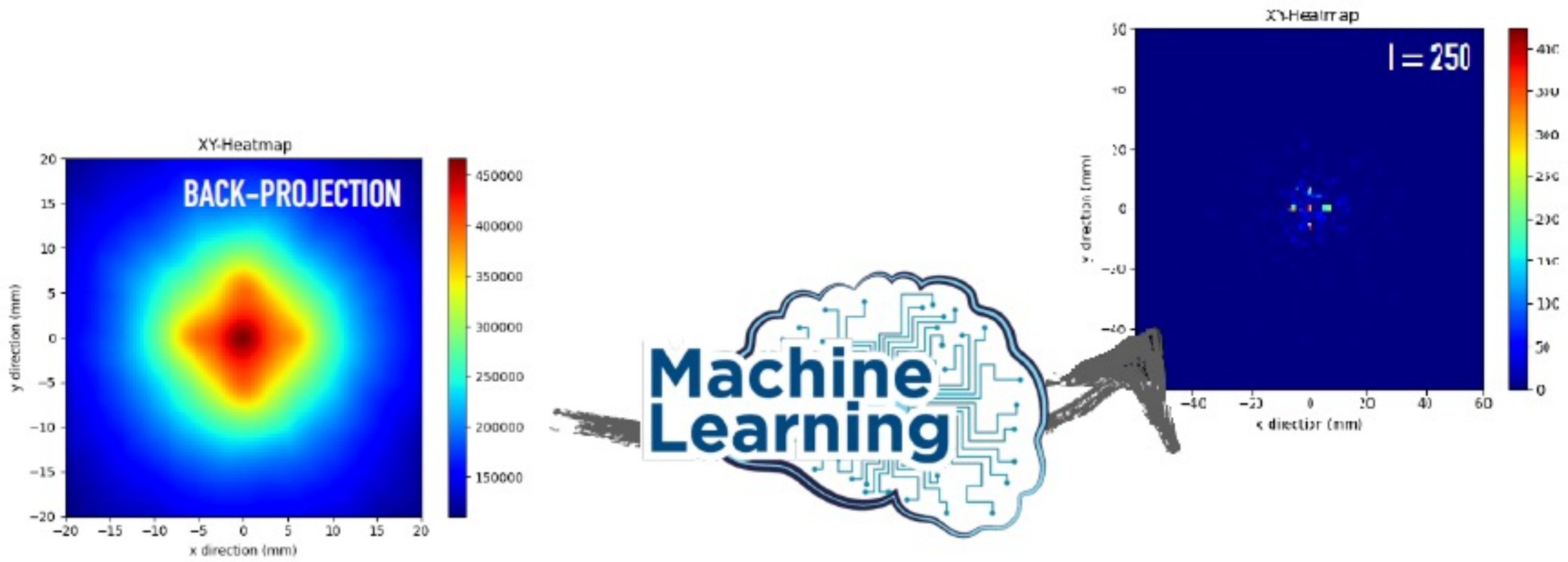

Training **Deep Learning** model with back-projection and tomography labels sets to make **tomography reconstruction**

Improve **MC simulations** and built a **more suitable database**

warning

No availability of Compton images databases within BNCT

Improved simulations

3 new configurations to improve the 3D imaging reconstruction (reduce stretching long z-axis):

- single module placed at a distance of 60 mm from cylinder axis,
- four modules (2 frontal and 2 at ±60°),
- six modules (4 frontal and 2 at ±60°)

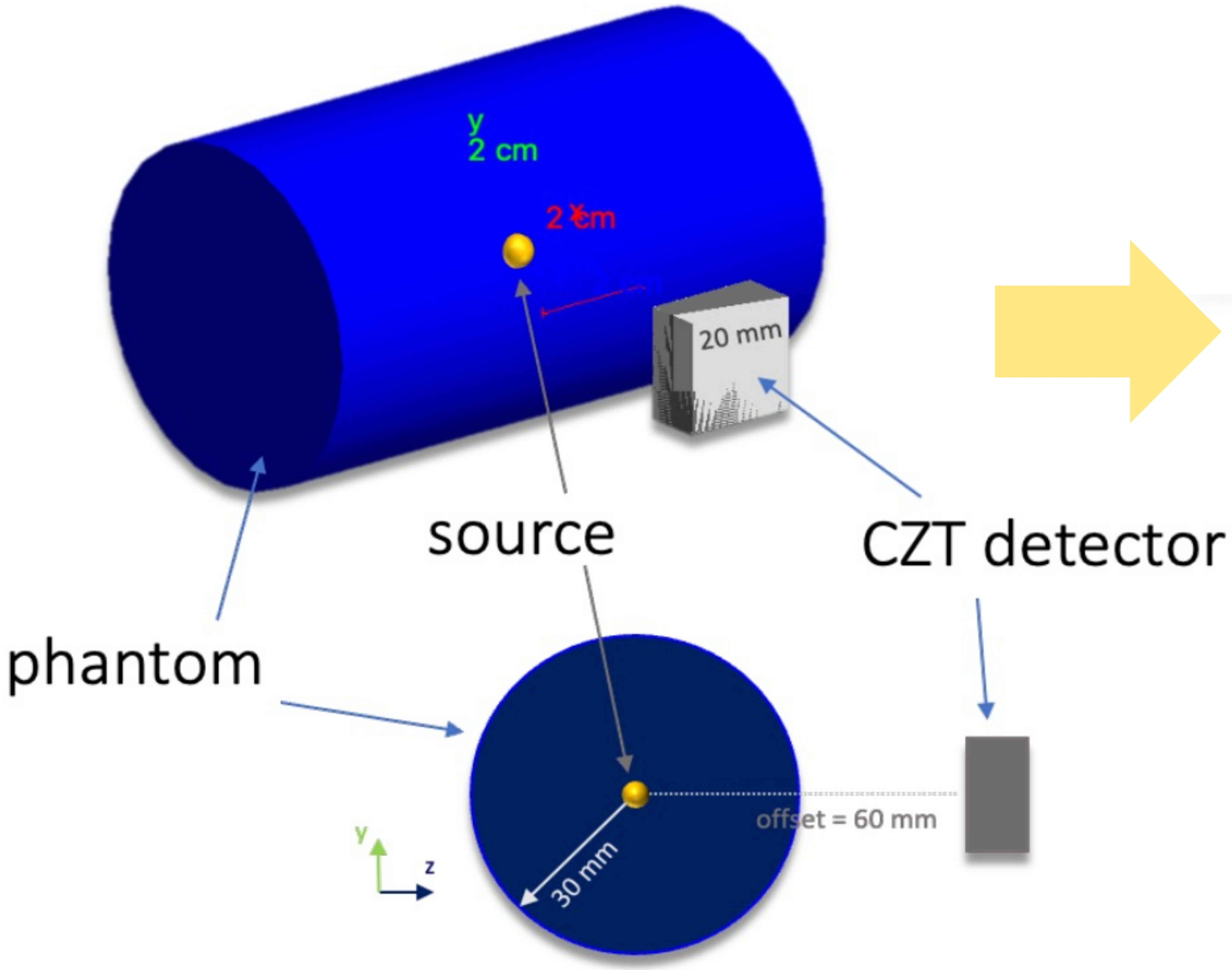

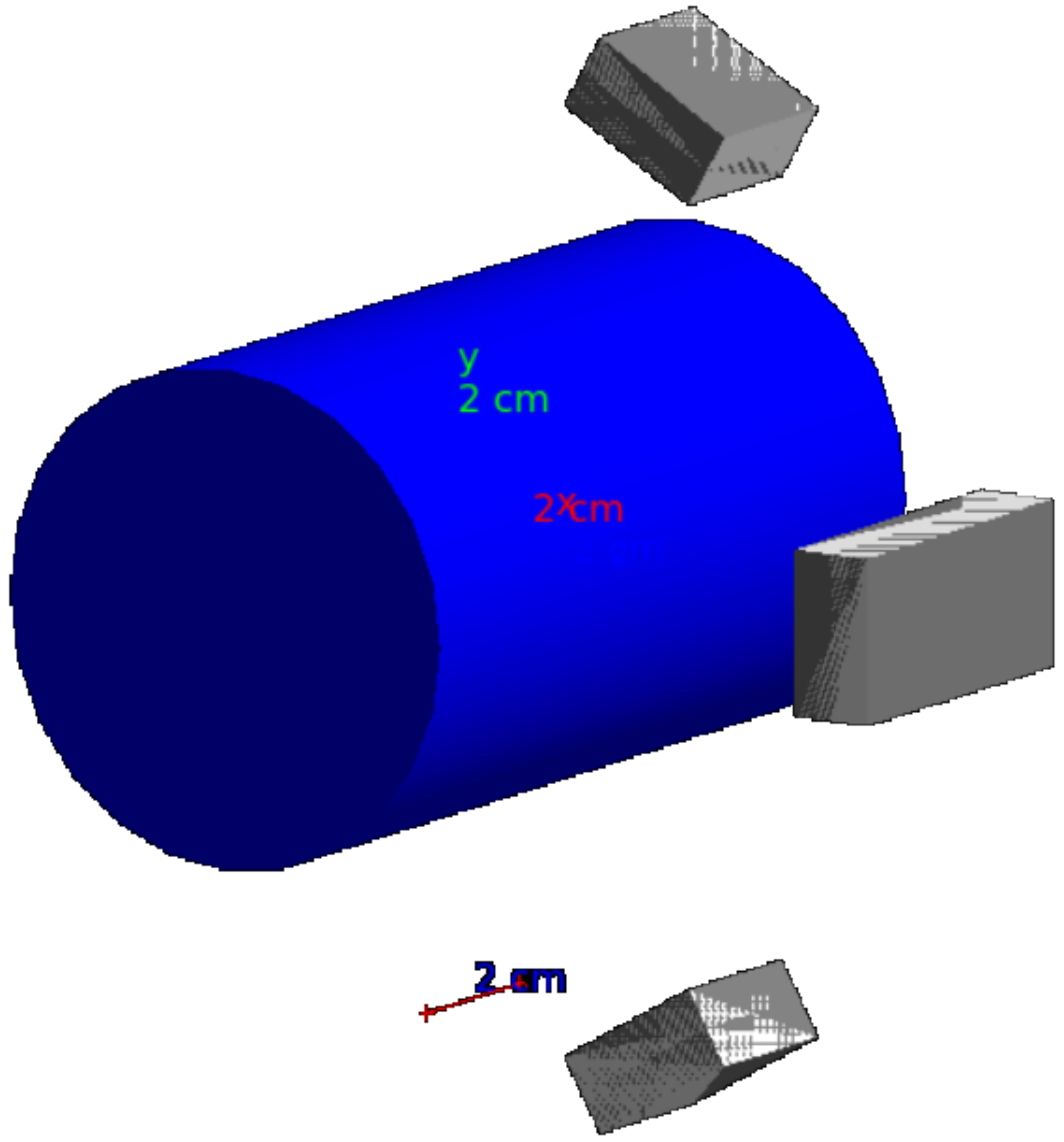

4 modules

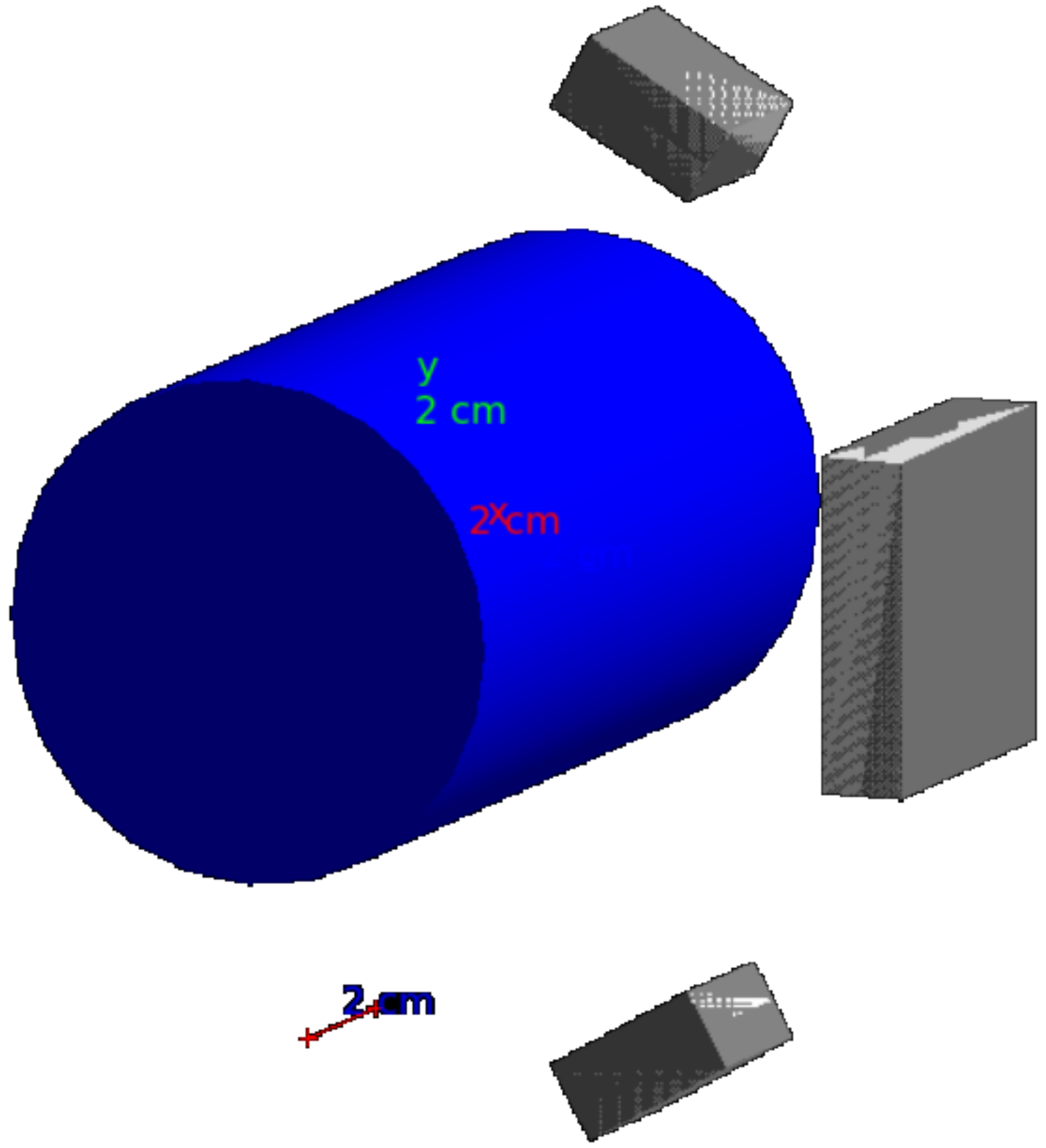

6 modules

Improved simulations

20 different tumor region shapes to obtain a suitable quantity of data for the training phase of deep neural network algorithms

U-Net model variants

- U-Net and improved versions used for image denoising*:

  (a) classical U-Net

  (b) dual frame U-Net

  (c) tight frame U-Net with Haar filter bank

- The input images are the results of the tenth iteration (~ 4-6 min) of MLEM algorithm

- The models were impletented in 3-D variants

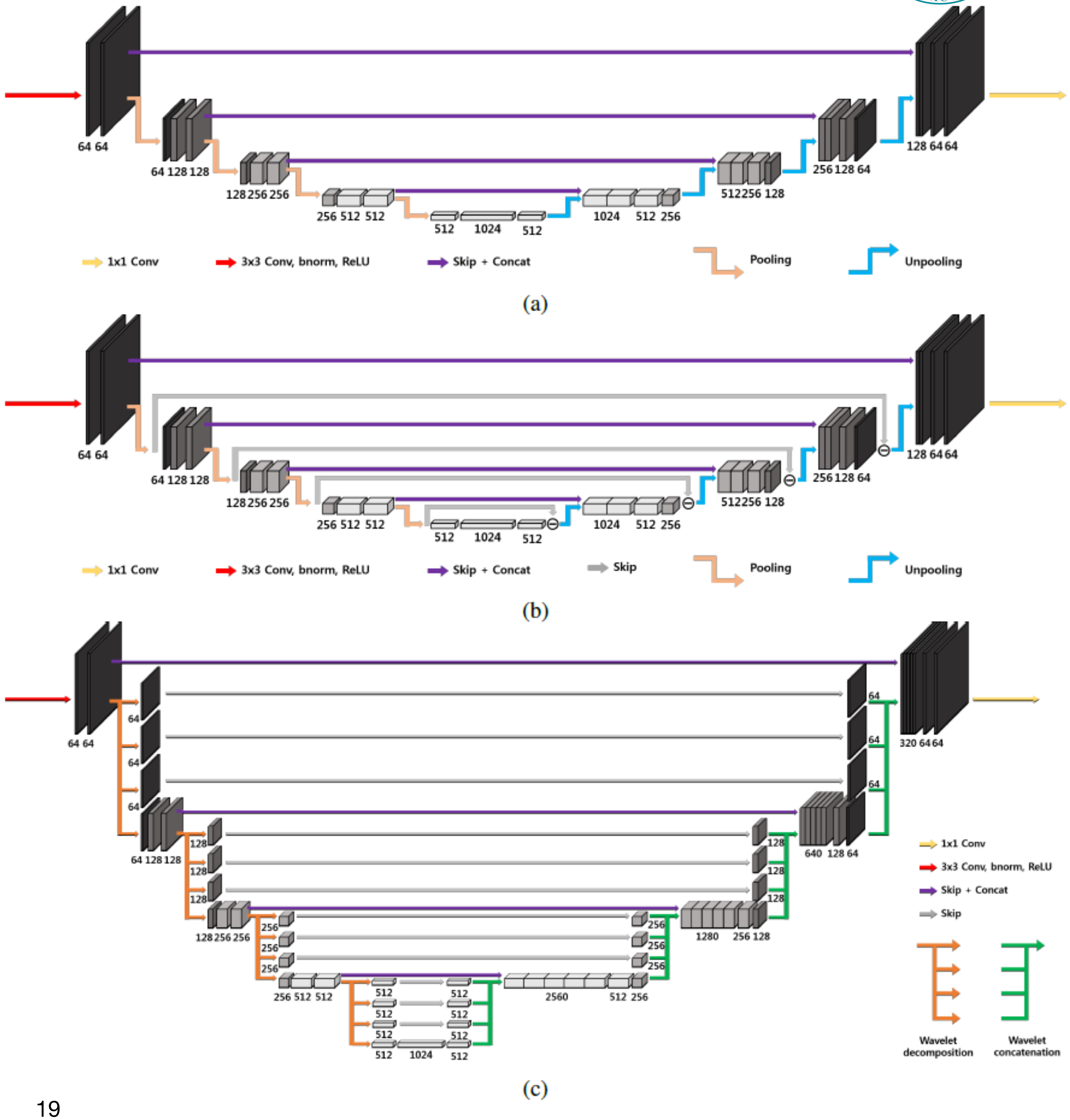

*Framing U-Net via Deep Convolutional Framelets: Application to Sparse-view CT Yoseob Han and Jong Chul Ye, Senior Member, IEEE

Evaluation

- Networks were trained using ADAM algorithm with learning rate 0.001 and NMSE loss function
- Evaluation: $NMSE = \frac{\|f^* - \hat{f}\|_2^2}{\|f^*\|_2^2}$ $\quad PSNR = 10\log_{10}\left(\frac{\|f^*\|_\infty{}^2}{MSE}\right)$ $\quad SSIM = \frac{(2\mu_{\hat{f}}\mu_{f^*} + c_1)(2\sigma_{\hat{f}f^*} + c_2)}{(\mu_{\hat{f}}^2 + \mu_{f^*}^2 + c_1)(\sigma_{\hat{f}}^2 + \sigma_{f^*}^2 + c_2)}$

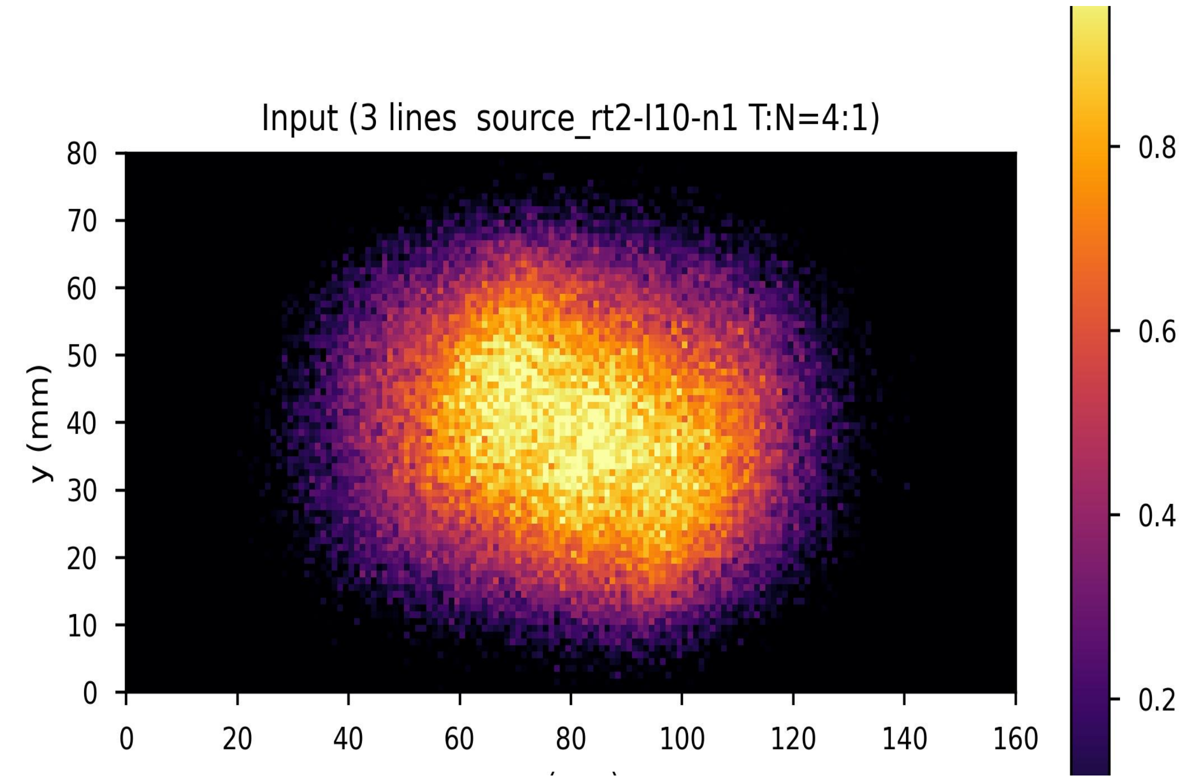

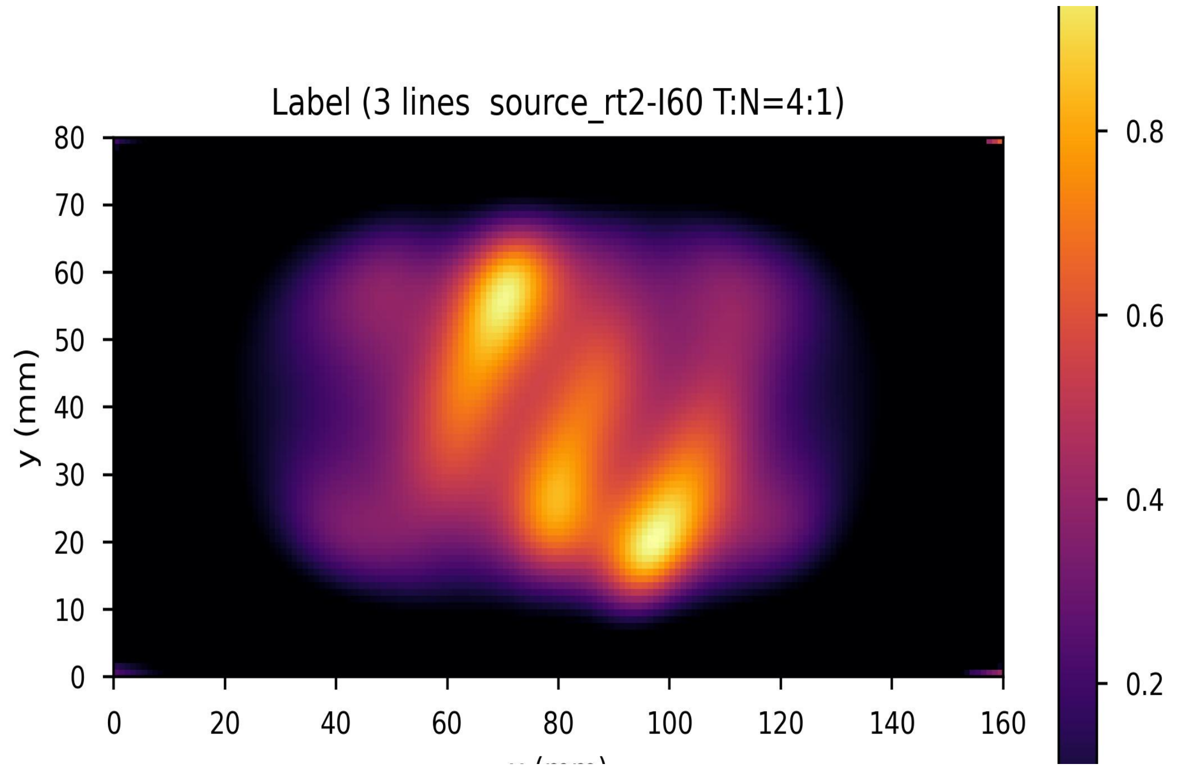

	NMSE	PSNR	SSIM
Standard U-Net	0.031803	36.119379	0.754417
Dual frame U-Net	0.029113	36.396008	0.726286
Tight frame U-Net	0.011953	40.615813	0.853548

Prediction time: ≈4-6 min

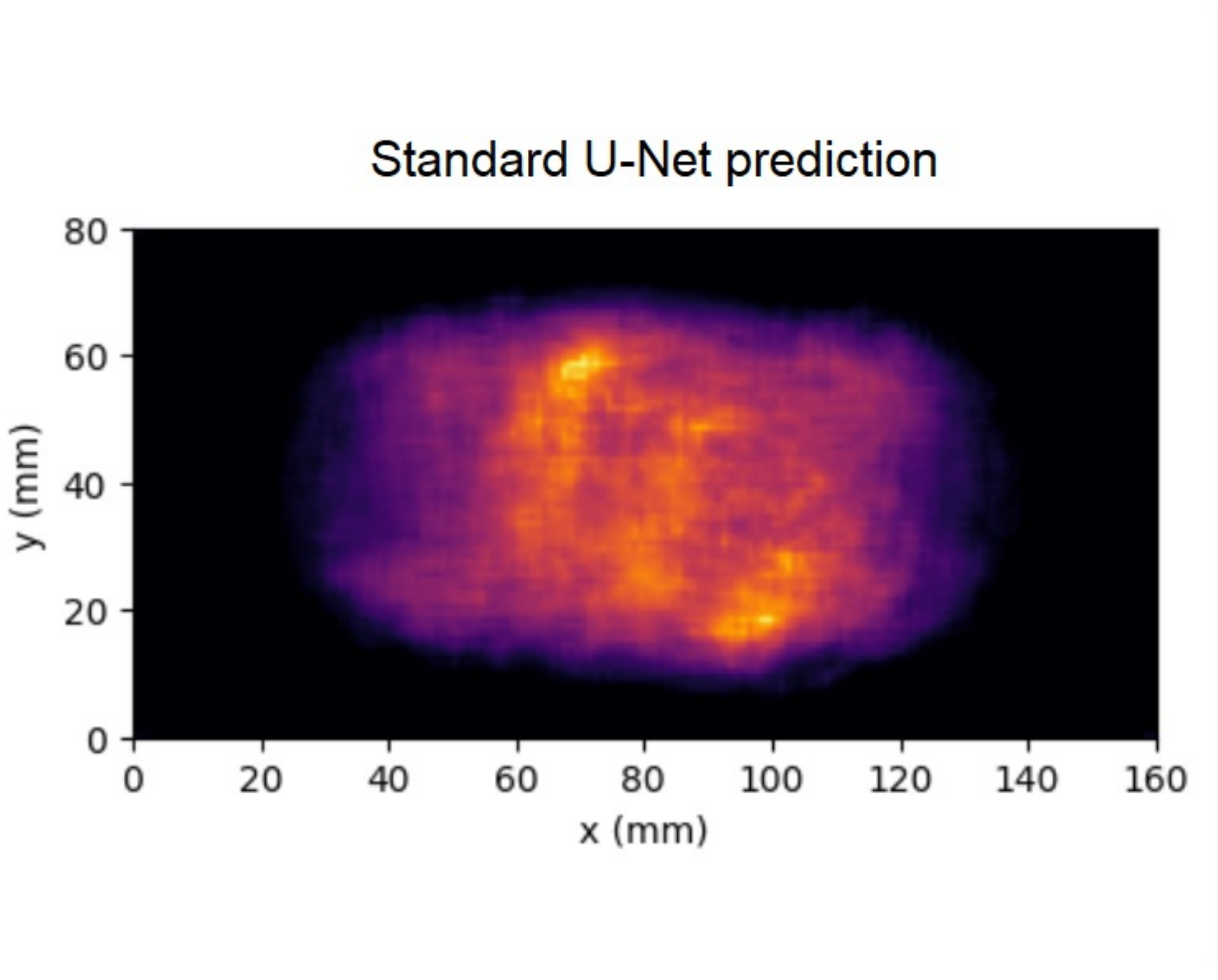

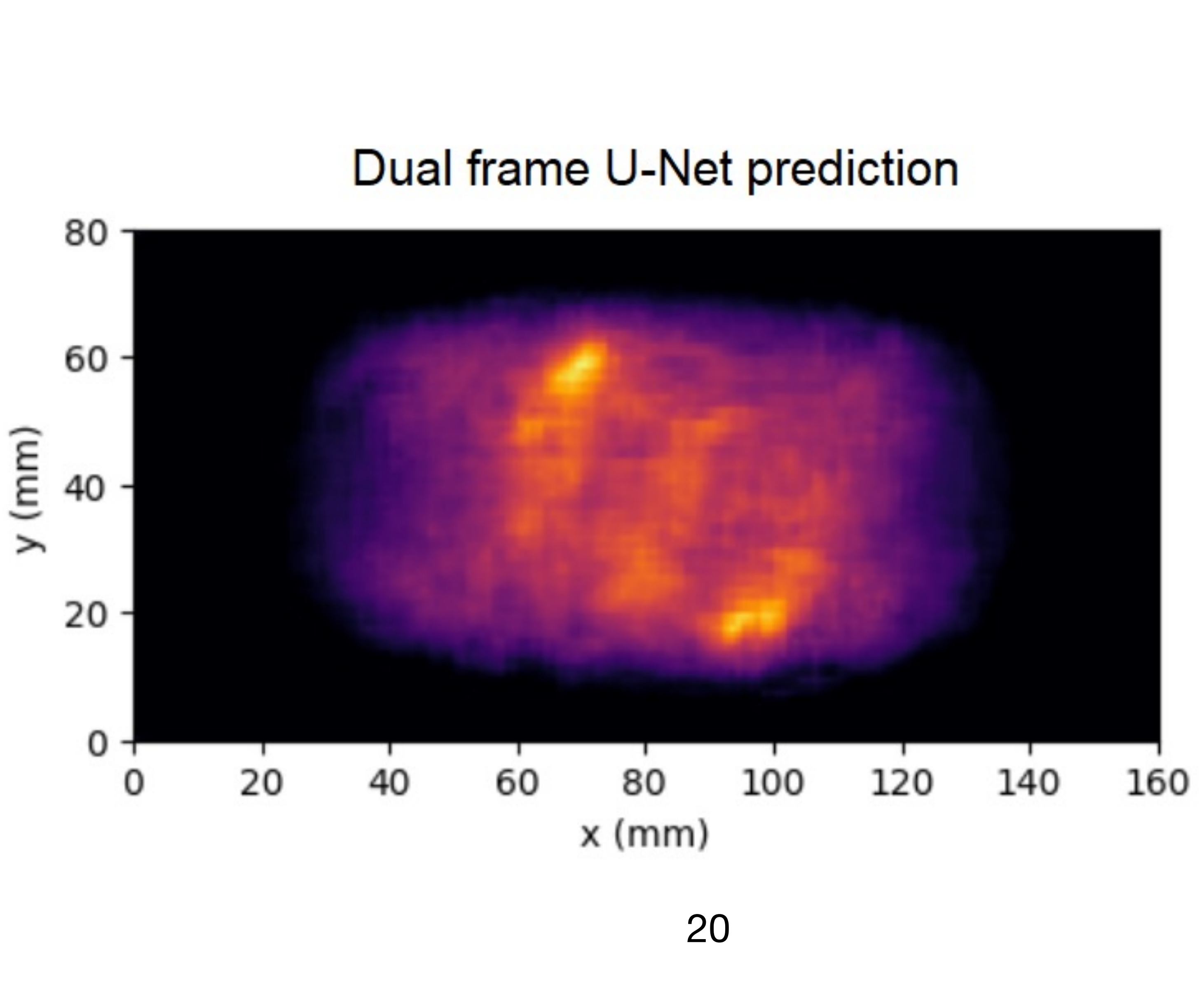

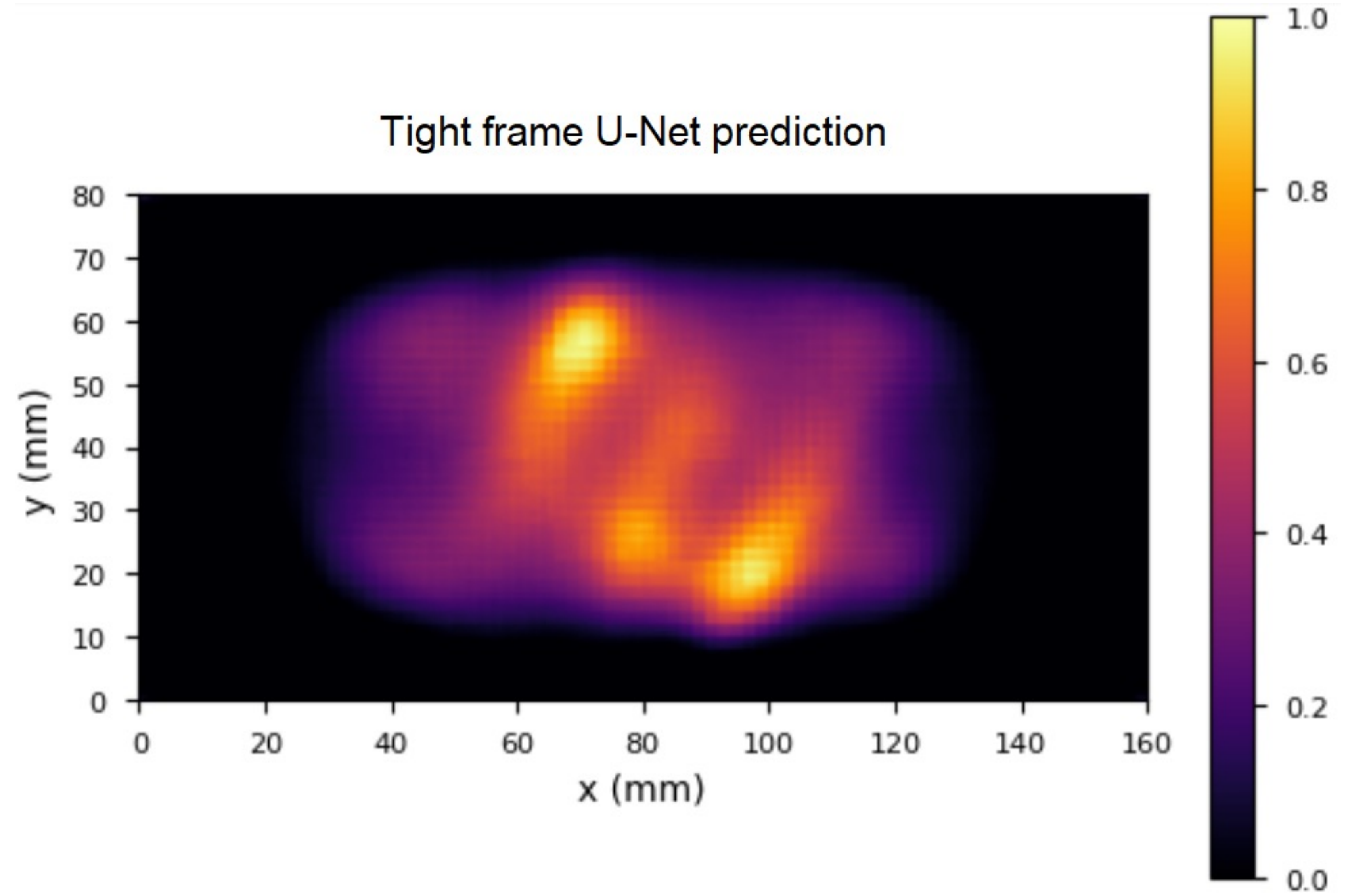

Summary and Future

- There is a possibility to exploit SPECT and Compton imaging approaches for boron dose tomography within Boron Neutron Capture Therapy

  Compton imaging pros: dynamic FOV, no collimation is needed, less system complexity

- Fine tuning by using experimental data is needed (SPECT ongoing, Compton imaging → founding for a prototype)
- The use of Deep Learning has proved the possibility to reduce reconstruction times (≈4-6 min using Compton imaging)

What's next?

- Development of Deep Learning algorithms to be applied to SPECT reconstruction
- Approaches to reduce artifacts and improve reconstruction, more detailed MC simulation, unrolled learned prior algorithm optimization, other deep learning techniques (GANs, DIP, ...)

Politecnico di Bari

INFN BARI
Istituto Nazionale di Fisica Nucleare
Sezione di Bari

SensIMed LABORATORY

Thanks!

dayron.ramos@ba.infn.it

ReCaS

DIPARTIMENTO INTERATENEO DI FISICA

Quasimodo
Quantum sensing for one-health

Spares

Tumor Monitoring DL model

- **Matlab pipe-line** for segmentation of images

- Use of Convolutional Neural Network model with a **Residual U-net Architecture (ResNet)**, widely used for segmentation

Test metrics: **accuracy and sensitivity**

$$Accuracy = \frac{TP}{TP + FP}$$

$$Sensitivity = \frac{TP}{TP + FN}$$

Resnet U-net architecture

Property	Value
Layers	206×1 Layer
Connections	227×2 table
InputNames	1×1 cell
OutputNames	1×1 cell

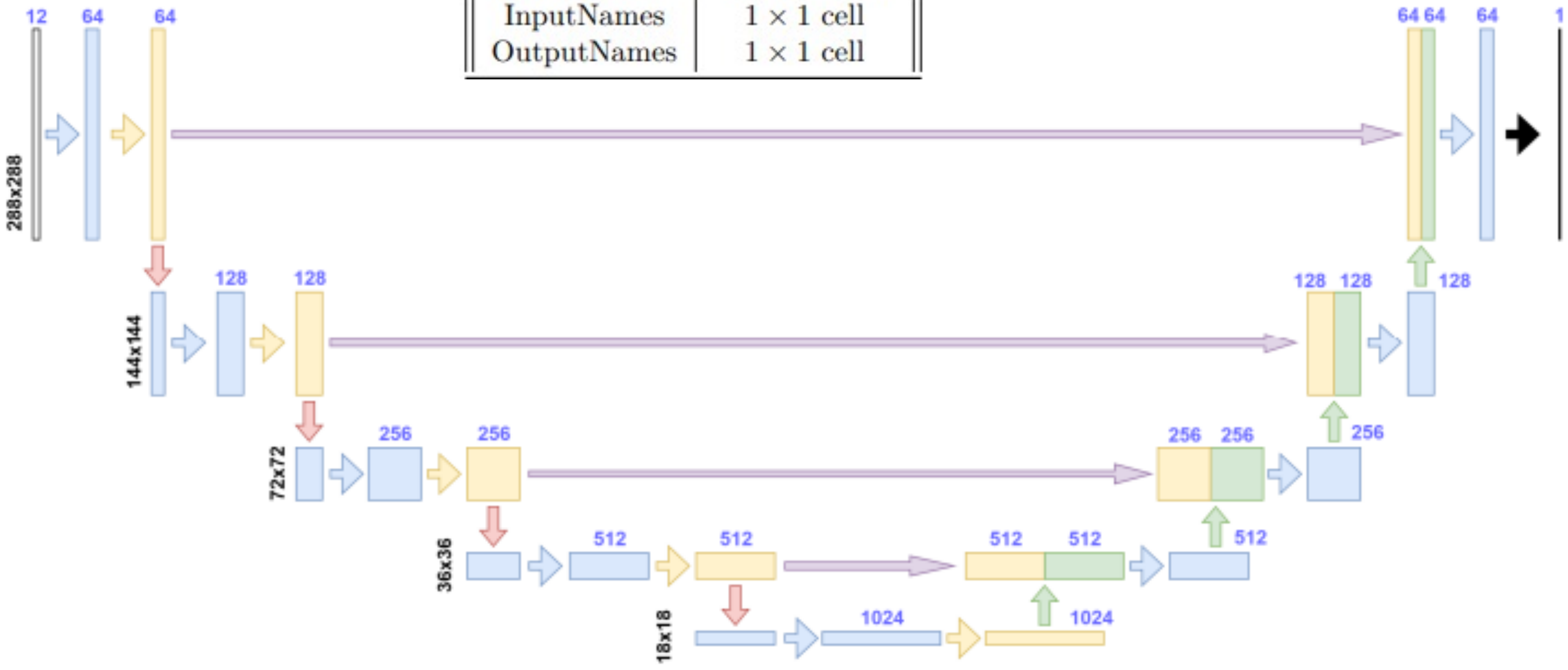

(a)

Model performance performance

	Accuracy	Sensitivity
case 1	79.56%	99.87%
case 2	4.83%	100%
case 3	19.68%	100%
case 4	3.81%	100%

Normalized back projections

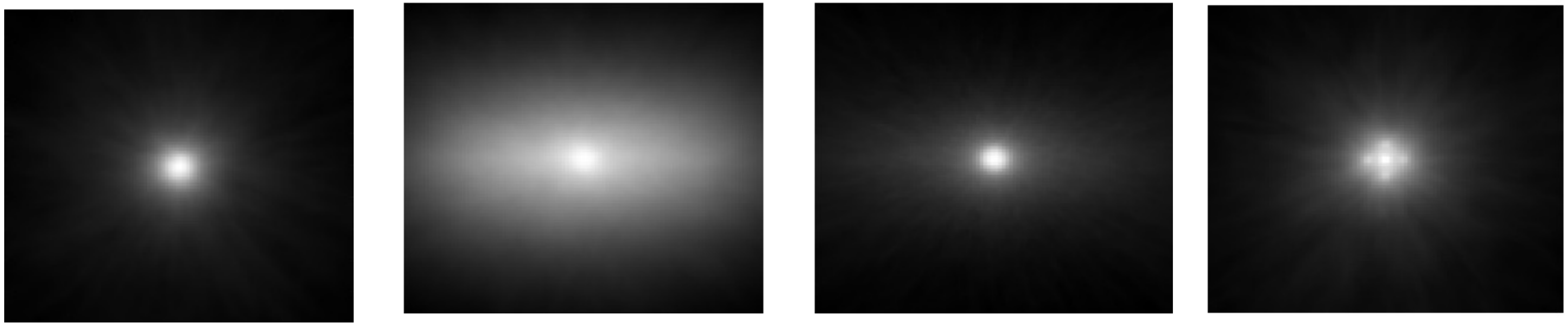

Case 1: Spheric source in Air

Case 2: Spheric source in Tissue (T/N=2)

Case 3 Spheric source in Tissue (T/N=5)

Case 4: 5 point-like source in air

ResNet segmentation

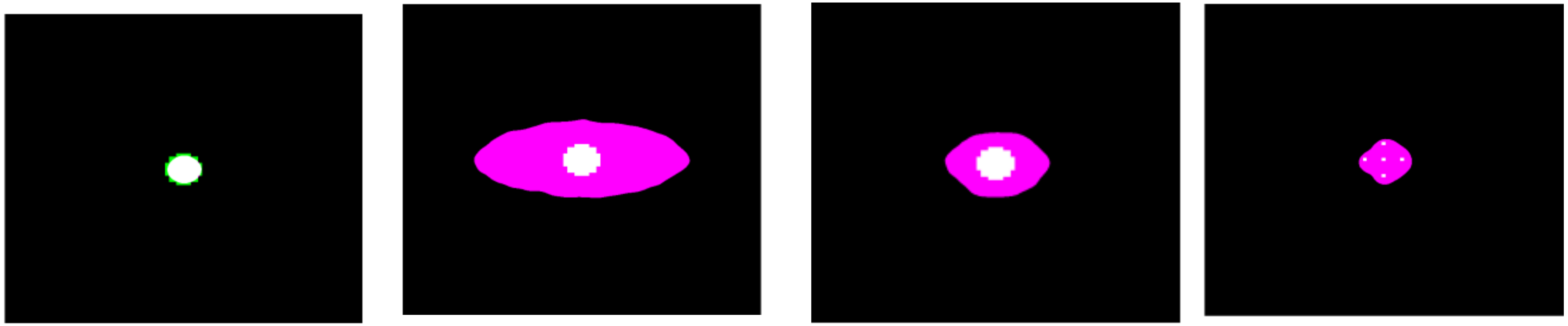

List-mode MLEM with single-view camera

Poor localization of the source in the z direction with single-view camera, although single-view reconstructions could be integrated with multi-view using image fusion techniques

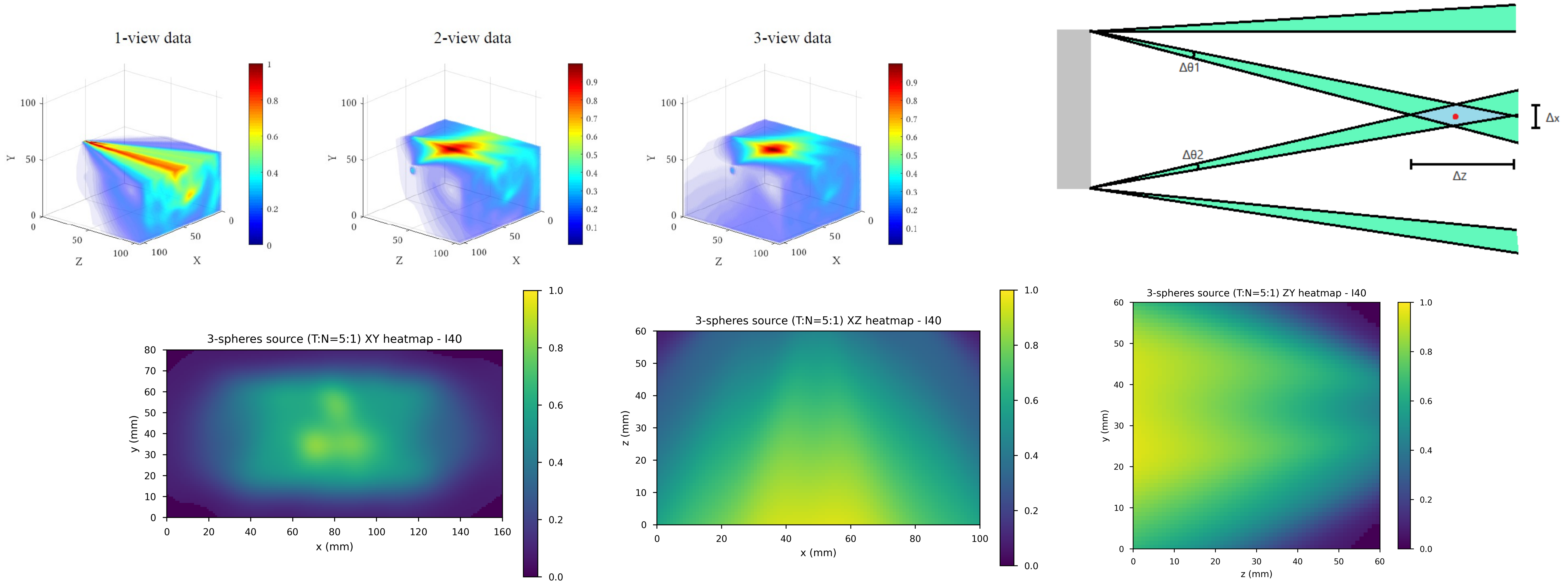

Dataset

- Starting from 20 different tumor source geometries, 71 original 3D images were obtained considering different T:N ratios (3:1, 4:1, 5:1, ∞:1). Input: 10th iteration MLEM reconstructions, output: 60th iteration reconstructions
- For each of the 71 original images, 4 roto-translations of the tumor source were considered (71x5 images)
- For each of the images, 41 images were obtained by adding four different levels of white Gaussian noise (71x5x42= 14910 images)
- Distributed 70 : 10 : 20 among the training set (11130 images), validation set (1260 images) and test set (2520 images)

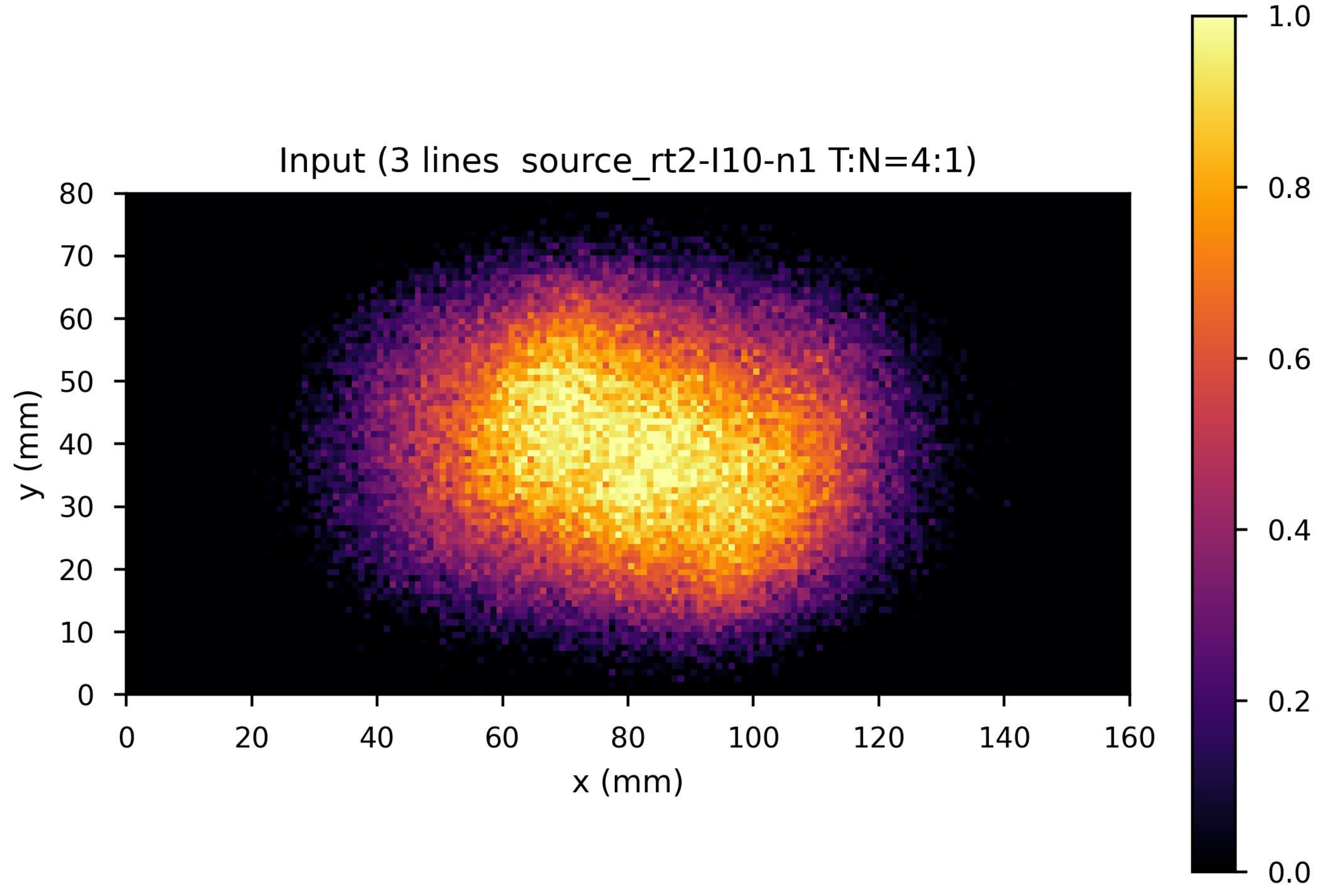

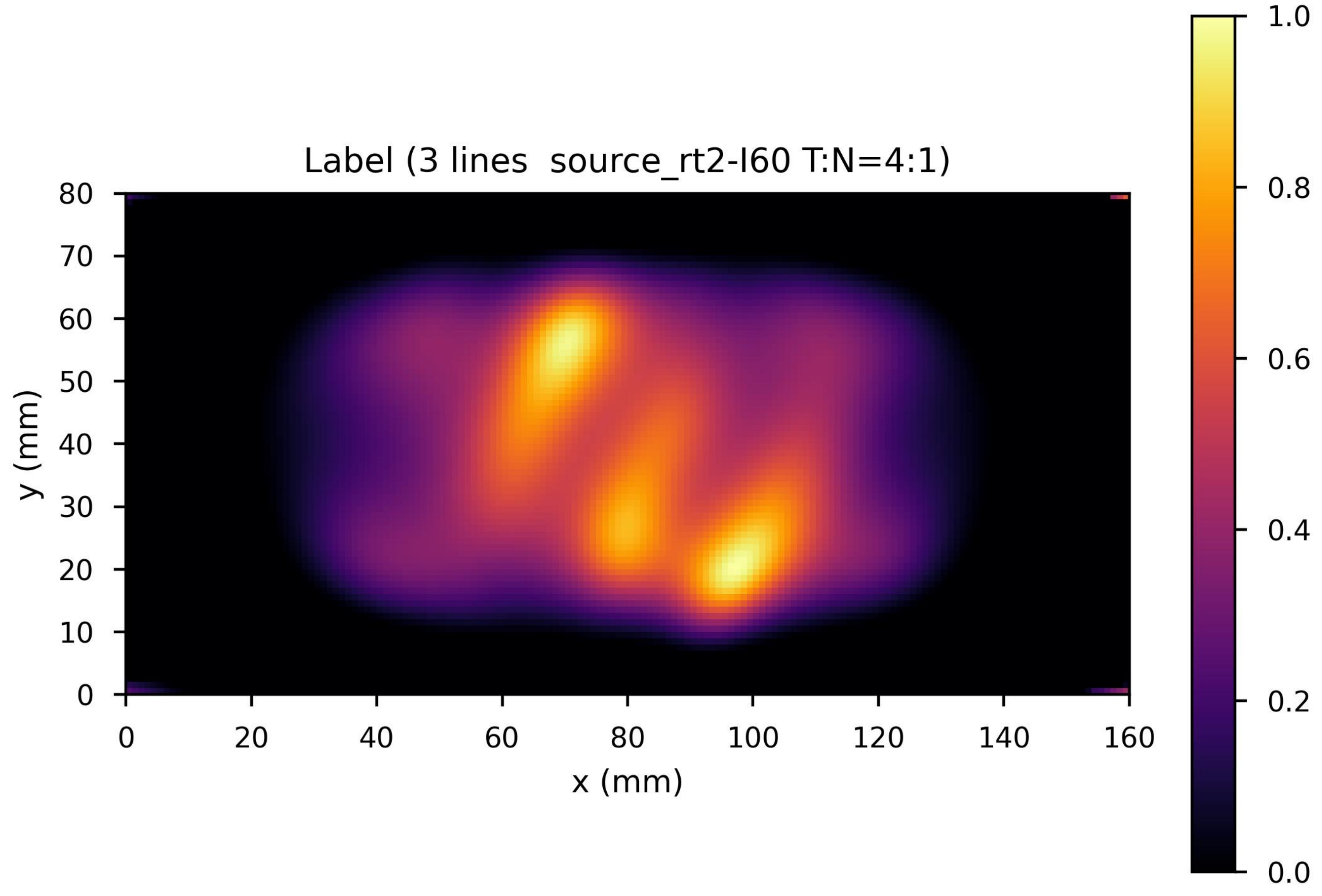

Training phase and evaluation

- Networks were trained using ADAM algorithm with learning rate 0.001 and NMSE loss function
- Evaluation: $NMSE = \frac{\|f^* - \hat{f}\|_2^2}{\|f^*\|_2^2}$ $PSNR = 10\log_{10}\left(\frac{\|f^*\|_\infty{}^2}{MSE}\right)$ $SSIM = \frac{(2\mu_{\hat{f}}\mu_{f^*} + c_1)(2\sigma_{\hat{f}f^*} + c_2)}{(\mu_{\hat{f}}^2 + \mu_{f^*}^2 + c_1)(\sigma_{\hat{f}}^2 + \sigma_{f^*}^2 + c_2)}$
- Prediction time: ≈4-6 min (BNCT treatment duration: ≈30-90 min, MLEM algorithm: ≈24-36 min) min

Network	n_{te}	Best epoch	Tr. NMSE	Val. NMSE
U-Net	56	39	0.03396	0.02865
Dual frame U-Net	53	50	0.03280	0.02571
Tight frame U-Net	52	48	0.01102	0.01113

	NMSE	PSNR	SSIM
Standard U-Net	0.031803	36.119379	0.754417
Dual frame U-Net	0.029113	36.396008	0.726286
Tight frame U-Net	0.011953	40.615813	0.853548